DOI: 10.1002/adma.200800604

# Low-Dimensional Nanomaterials Based on Small Organic Molecules: Preparation and Optoelectronic Properties**

By *Yong Sheng Zhao, Hongbing Fu, Aidong Peng, Ying Ma, Debao Xiao,* and *Jiannian Yao**

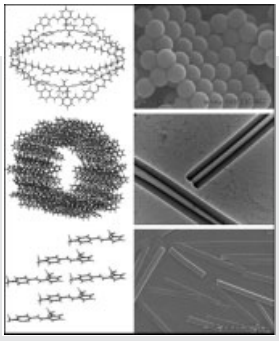

*This article presents a comprehensive review of recent progress of research dedicated to low-dimensional nanomaterials constructed from functional low-molecular-weight organic compounds, whose optoelectronic properties are fundamentally different from those of their inorganic counterparts. After introducing the development of inorganic and organic macromolecular nanomaterials, we begin with a general review of the construction strategies for achieving both zero-dimensional (0D) and one-dimensional (1D) nanostructures from small organic functional molecules. We then provide an overview of the unique optoelectronic properties induced by molecular aggregation in the nanostructures. Special emphasis is put on the luminescent properties that are different from those of the corresponding bulk materials, such as aggregation-induced enhanced emission, fluorescence narrowing, multicolor emission, and tunable and switchable emissions from doped nanostructures. We conclude with a summary and our personal view of the direction of future development of organic opto-functional nanomaterials and devices.*

## 1. Introduction

During the past two decades, more and more research attention has been paid to nanomaterials — those functional materials composed of objects with at least one of the three dimensions in the range 1–100 nm. Owing to their surface effect,[1] quantum size effect,[2] macroscopic quantum tunneling effect,[3] and so on, nanomaterials exhibit unique properties superior to those of their bulk counterparts.[4–7] In addition, the unique size-dependent optoelectronic properties[8,9] of nanomaterials has made them of significant use in areas such as highly efficient catalysis,[10] bio-labeling[11,12] and functionalization,[13,14] novel luminescent materials,[15–17] nonlinear optics,[18,19] chemical sensors,[20,21] and super high density information storage.[22]

If hybrids are neglected, nanomaterials can be divided into inorganic materials, organic macromolecular materials, and those based on organic low-molecular-weight compounds, from the viewpoint of chemical composition, of which, inorganic nanomaterials have been most widely investigated from the very beginning of the rise of nanoscience. Zero-dimensional (0D) inorganic nanostructures, including nanoparticles, clusters, and quantum dots, have been well studied by researchers all over the world. For example, work on the preparation,[23–25] shape control,[26] and size-dependent optoelectronic properties[27] of semiconductor quantum dots has been reported by many groups. Quantum dots have also been used to prepare various nanodevices, such as light-emitting diodes,[17] solar cells,[28]

[*] Prof. J. N. Yao, Dr. Y. S. Zhao, H. B. Fu, A. D. Peng, Y. Ma, D. B. Xiao
Center for Molecular Science
Institute of Chemistry, Chinese Academy of Sciences
Beijing 100080 (P. R. China)
E-mail: jnyao@iccas.ac.cn
Dr. Y. S. Zhao
Graduate School, Chinese Academy of Sciences
Beijing 100039 (P. R. China)

[**] This work was supported by the National Natural Science Foundation of China (nos. 50221201, 90301010, 20733006, 50573084), the National Research Fund for Fundamental Key Project No. 973 (2006CB806200), and the Chinese Academy of Sciences.

chemical sensors,[29] and photodetectors,[30] and for data storage.[31] Another important area of 0D inorganic nanomaterials is metal[32,33] and magnetic compound nanoparticles[34,35] for bio-applications. Since the discovery of carbon nanotubes in 1991,[36] 1D nanomaterials, including wires,[37,38] tubes,[39,40] rods,[41] and belts,[42] have also attracted extensive research interest, because it was realized that, compared with their 0D counterparts, 1D structures are more suitable for the construction of active nanodevices and interconnects due to the 2D quantum confinement effect. Inorganic 1D nanostructures have revealed their promising applications as building blocks for nanoscale devices, such as waveguides,[38,43,44] lasers,[45,46] and sensors.[47] Lieber,[48] Xia,[49] Yang[49,50] and coworkers have successively provided several detailed reviews of the fabrication and properties of inorganic 1D nanostructures. 2D inorganic nanostructures, including super-thin films, multilayered films, and superlattices, are also known as quantum wells and have been prepared, mainly by molecular beam epitaxy (MBE), and widely investigated.[51]

Besides inorganic nanomaterials, those composed of organic macromolecules — polymers, biomolecules, graphene molecules, dendrimers, etc. — have also been investigated extensively during the past decade. In the 0D area, monodisperse polystyrene nano- and microspheres[52,53] have been widely documented for the construction of photonic crystals. Nanospheres can also be obtained from conjugated polymers[54,55] or block copolymers[56,57] by self-assembly and miniemulsion processes in solution. Macromolecular 1D nanostructures have also been widely studied. First, 1D micro/nanostructured conductive polymers, such as polyaniline[58] and polypyrrole,[59] attracted growing attention because of their good electrical conductivity, redox properties, environmental stability, and potential applications in sensors,[60] biomedicine,[61] actuators,[62] etc. Second, 1D nanostructures based on semiconductor conjugated polymers, such as polyfluorene (PF), polythiophene (PT), polyphenylenevinylene (PPV), are attracting significant research interest, owing to their many novel optoelectronic properties and applications such as field effect transistors,[63] optically pumped lasers,[64] photodetectors,[65] and electroluminescent diodes.[66] The most commonly adopted preparation methods for polymer 1D nanostructures include electrochemical deposition,[67] electrospinning,[68] self-assembly,[69] and the template method.[70] Finally, thanks to the development of supramolecular chemistry, some macromolecules other than polymers have also been used to form 1D nanostructures, mainly by self-assembly. For example, DNA molecules were used not only to synthesize nanowires,[71] but also to prepare[72] and modify nanostructures of other materials.[73] Ghadiri and coworkers pioneered the work of constructing hollow tubular structures from another kind of biomacromolecules, cyclopeptides,[74,75] while Meijer and coworkers[76] and Grimsdale and Müllen[77] studied the chemistry and electronic properties of the nanostructures prepared from a series of $\pi$-conjugated systems, especially graphene molecules, those molecules containing multi-acenes. Dendritic macromolecules[78–80] and some amphiphilic long-chain molecules[81] were also successfully designed for the synthesis of tubular structures through self-assembly in solutions.

*Jiannian Yao was born in Fujian, P. R. China, in 1953. He was awarded his B.S. degree in chemistry from Fujian Normal University of China in 1982. After that, he worked at the same university as a lecturer for five years. In 1988, he went to Japan to work with Prof. Akira Fujishima at Tokyo University, receiving his M.E. in 1990 and his Ph.D. in 1993. In 1995 he became an associate professor in the Institute of Photographic Chemistry, Chinese Academy of Sciences (CAS), and was promoted to full professor in 1996. In 1999 he joined the Institute of Chemistry, CAS, as a professor and deputy director. He is currently serving as a permanent member and general secretary of the Chinese Chemical Society. His research interests are focused on organic nanomaterials and inorganic optofunctional materials with photochromic and photocatalytic properties.*

*Yong Sheng Zhao was born in Shandong, P. R. China, in 1979. He received his B.E. degree in chemical engineering from Qingdao University of China in 2000. From 2000 to 2003 he studied under Prof. Zhengzhi Pang at Beijing University of Chemical Technology (BUCT), and was awarded his M.S. degree in polymer chemistry and physics. In 2003 he joined Prof. Jiannian Yao's group at the Institute of Chemistry, CAS, where he obtained his Ph.D. in physical chemistry in 2006. After that, he went to Prof. Qibing Pei's laboratory as a postdoctoral fellow at the University of California at Los Angeles (UCLA), and then joined Prof. Jiaxing Huang's group at Northwestern University in 2008. His research interests include photonic and optoelectronic properties of organic nanomaterials and organic/inorganic hybrid nanomaterials.*

Unlike their inorganic and macromolecular counterparts, nanomaterials based on traditional functional small organic molecules have been the subject of research interest only in recent years, which may be ascribed to two primary factors. First, owing to their lower melting temperatures, thermal instability, and poorer mechanical properties compared to inorganic materials, there are fewer routes for fabricating small organic compounds into nanostructures. Especially, the top-down strategy for producing inorganic nanostructures is difficult to apply to organic materials. Second, until recently, size-dependent optical and electronic properties were not anticipated in organic nanomaterials because, unlike the case of Wannier excitons[82] in inorganic semiconductor and metal crystals, the optoelectronic properties of organic crystals are determined by charge transfer (CT) excitons[83] and Frenkel excitons with smaller radius.[84] However, with a deeper understanding of organic materials, great changes have occurred in both factors that hamper the development of organic nanomaterials. After reprecipitation[85] was first applied by Nakanishi and coworkers as a facile method to prepare organic nanoparticles, more and more strategies have been developed for constructing organic nanostructures with different morphologies, crystallinities, and optoelectronic properties. During this process, it was noticed that many properties also exhibit an obvious size effect in aggregates of organic molecules. For example, Chernyak et al. proved the aggregate size-dependence of Stokes shift of the molecular spectra.[86] It was also found that the limitation of the molecular exchange interactions results in an increase of the nonlinear optical properties in organic aggregates.[87] That the melting point of organic nanocrystals is size dependent was also proved both theoretically and experimentally.[88] Furthermore, because the intermolecular interactions in organic materials are of weak types, such as hydrogen bonds, $\pi$-$\pi$ stacking, and van der Waals contacts, it was observed that the optical and electronic properties of organic nanomaterials are fundamentally different from those of inorganic materials. As a consequence of the variety, multifunctionality, designability, and tailorability of small-organic nanomaterials, ever more work is being carried out to extend research on nanostructured materials into the small organic area.

This article reviews recent research work that focuses on low-dimensional nanoscale materials based on functional small organic molecules. In Section 2, we review the strategies that have been developed for achieving organic nanostructures. The preparation methods for 0D and 1D organic nanostructures are discussed in detail. In the next section, the unique optoelectronic properties of organic nanomaterials are introduced, and more attention is paid to the novel luminescent behavior. At the end, we provide a conclusion and our personal view of the future development of research in this area.

## 2. Construction of Organic Nanostructures

The preparation of 0D organic nanoparticles, especially those dispersed in aqueous solutions, was treated in detail in the review by Horn and Rieger[89] published in 2001, which summarized several methods, including emulsification–evaporation,[90,91] emulsification–diffusion,[92,93] the supercritical fluids method,[94,95] and the polyelectrolyte complexes method.[96,97] Therefore, in this section, we just introduce the recent progress on the fabrication of organic nanoparticles, and then deal with the construction of 1D organic nanostructures in more detail.

### 2.1. Methods for the Production of 0D Organic Nanoparticles

Most of the current work focuses on organic nanoparticles with a single chemical composition dispersed in an aqueous system. Of all the preparation methods, reprecipitation is the most facile and commonly used one, although sometimes laser ablation,[98] microwaves,[99] a microemulsion,[100] and a membrane reactor,[101] etc. were used to assist the formation of nanoparticles in the aqueous surroundings. In addition, the self-assembly of organic nanoparticles was also studied, and hybrid nanoparticles were also obtained, either by blending two kinds of small molecules or as a composite of small molecules and polymers.

#### *2.1.1. Reprecipitation*

Reprecipitation, which is a solvent displacement method, was first reported by Nakanishi and coworkers.[85,102,103] It provides a very simple and versatile way to prepare organic nanoparticle dispersions. The method involves a rapid mixing of a small amount of concentrated stock solution of the target compound dissolved in a good solvent with excess of a poor solvent. The great disparity between the solubilities of the target compound in the good and poor solvents and the good compatibility of the two solvents are essential for this method. It is supposed that the rapid mixing of the stock solution and the poor solvent changes the micro-environment of the target compound molecules. The molecules are exposed to the poor solvent surroundings in a very short time, inducing the nucleation and growth of the molecules to nanoparticles.

With this method, a series of organic nanoparticles were successfully fabricated by several groups. For example, after their pioneer work on this method, Nakanishi and coworkers prepared perylene nanoparticles and observed the emissions from both free excitons and self-trapped excitons.[104,105] Horn and coworkers prepared nanoparticles from $\beta$-carotene and observed the influence of both supramolecular structure and particle size on the absorption spectra.[106] Majima's group[107] and Barbara's group[108] prepared nanocrystals from perylene and a perylene derivative, respectively, and studied the spectroscopy of single nanoparticles. The size dependence of the luminescence and the enhanced emission of the nanoparticles prepared with this method studied in Yao's group and Park's group will be discussed in detail in Section 3.

  

### 2.1.2. Chemical Reaction Method

Although reprecipitation is a facile approach to organic nanoparticles, it is difficult to form kinetically stable nanoparticle dispersions. In addition, large-scale synthesis is limited by the solubility of the target compound in the good solvent. Moreover, the heterogeneous environment of this method makes it difficult to precisely control the complicated nucleation process in the initial stages and the subsequent fast growth.[109] Consequently, the broad distribution in both size and shape of the organic nanoparticles generated using this method prevents them from acting as building blocks for further self-organization.

Recently, Yao and coworkers developed a colloid chemical reaction method to overcome these problems.[110] With this method, the perylene nanoparticles were prepared by the reduction of perylene perchlorate by $Br^-$ anions[111] in the presence of cetyl trimethylammonium bromide (CTAB) in acetonitrile. The large-scale synthesis of perylene nanoparticles ranging from 25 to 90 nm with a polydispersity of <10% was achieved by changing $N$, the molar ratio of CTAB to perylene perchlorate. Furthermore, the hierarchical self-organization of 25 nm perylene nanoparticles was observed, forming nanobelts and/or square nanorods when $N$ was increased above 1.0. Figure 1 displays the formation and hierarchical self-organization processes of the perylene nanoparticles. The homogeneous solution phase in this method provides several advantages, including facile separation of the nucleation and growth stages and better controllability of the growth parameters, through which size control of the organic nanoparticles was realized.

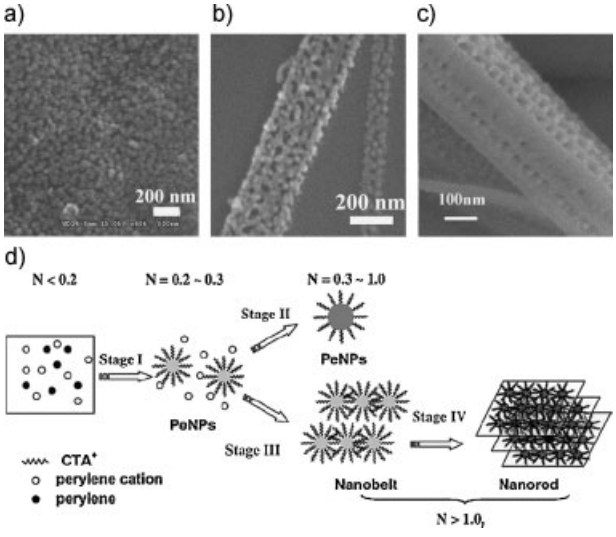


**Figure 1.** a) SEM image of quasi-spherical perylene nanoparticles with a size of ~25 nm at $N = 0.3$. b,c) The self-organization of the particles to nanobelts at $1.0 < N < 1.2$, and to square nanorods at $N > 2.0$. d) Schematic illustration representing formation of the perylene nanoparticles. Stage I, nucleation; stage II, growth; stages III and IV, 1D to 3D organization. (Reprinted from [110]. Copyright 2007 American Chemical Society.)

### 2.1.3. Fabrication of Composite Organic Nanoparticles

Composite materials, that is, materials made of two or more constituent materials with significantly different physical or chemical properties, may introduce brand new properties by means of synergistic effects between the constituents, besides retaining the properties of each constituent.[112] Composite organic nanoparticles with different structures have attracted increasing attention in recent years. Here we introduce the nanoparticles with core/shell structures, while the tunable emission properties of uniformly doped organic nanoparticles will be discussed in Section 3.

Jang and Oh fabricated pyrene/polypyrrole core/shell nanoparticles using microemulsion micelles as nanoreactors.[113] The mixture of pyrene and pyrrole monomers was dissolved in the hydrophobic interior of micelles formed in a surfactant solution, then the polymerization of the pyrrole monomers was initiated with ferric chloride. The polymerization induced phase separation between the polypyrrole and pyrene. It was considered that the enhanced hydrophobicity with increasing pyrene content facilitated the phase separation. In the nanoparticles loaded with a small amount of pyrene, the hydrophobic interaction between pyrene molecules is weak due to the relatively large distance, therefore, the aggregation of pyrene molecules was restrained and discrete pyrene molecules were trapped by crosslinked polypyrrole chains. With an increase of the amount of pyrene, the aggregation of pyrene molecules became inevitable. The change of the aggregation state caused the emission color of the composite nanoparticles to change from violet (pyrene monomer emission) to blue (pyrene excimer emission). Figure 2 shows the formation mechanism of the core/shell nanostructures and emission from the nanoparticles with different pyrene contents. Composite nanoparticles with different emission colors can be obtained by doping with different organic fluorescent dyes.

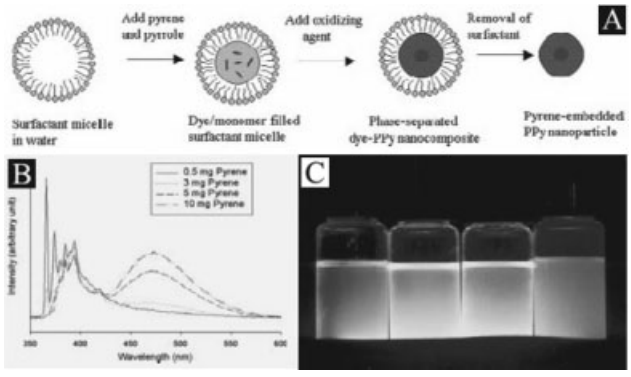


**Figure 2.** a) Schematic representation of the fabrication of polypyrrole nanoparticles with embedded pyrene. b) The photoluminescence spectra of pyrene-embedded polypyrrole nanoparticles for different pyrene loadings. c) Corresponding photograph (from left to right, the pyrene amounts are 0.5, 3, 5 and 10 mg). (Reprinted from [113].)

### 2.2. Methods for the Construction of 1D Organic Nanostructures

As was mentioned in Section 1, compared with their 0D counterparts, 1D nanomaterials are more suitable for the construction of active nanodevices and interconnects. It has been realized that the development of facile, mild, and widely applicable methods for the construction of organic 1D nanostructures is of great scientific and technical significance. Most of the present approaches to inorganic 1D nanomaterials are not applicable to organic nanomaterials because of their lower melting points and thermal instability. However, some fruitful attempts have been made in this area during the past couple of years.

#### *2.2.1. Self-Assembly in the Liquid Phase*

Almost everything has the inclination to self-assemble. Molecular self-assembly is a strategy for nanofabrication that involves designing molecules and supramolecular entities.[114] The assembly of organic molecules to nanostructures needs the driving forces from the molecules themselves and sometimes initiation from the surroundings. For example, Shelnutt and coworkers prepared porphyrin nanotubes by ionic self-assembly of two oppositely charged porphyrins in aqueous solution and investigated the photocatylytic behavior of the nanotubes.[115,116] Takazawa et al. induced the self-assembly of 3-ethyl-2-[(3-ethyl-2(3*H*)-benzothiazolylidene)-methyl]benzothiazolium iodide to form wire structures by cooling the hot solutions, and then studied the optical waveguiding behavior of the wires.[117,118] Shimizu and coworkers fabricated nanotubes by the self-assembly of amphiphilic molecules in solutions.[119]

Recently, Yao and co-workers reported the fabrication of single-crystalline nano- and sub-micrometer tubes by inducing the self-assembly of the small organic functional molecules 2,4,5-triphenylimidazole (TPI) in water at different temperatures.[120] Typical scanning electron microscopy (SEM) and transmission electron microscopy (TEM) images and the selected area electron diffraction (SAED) pattern of TPI tubes are shown in Figure 3. It can be seen that the TPI tubes have comparatively high monodispersity and open-ended structures. Each tube is single crystalline and the tube axis is the *c*-axis of the TPI crystal. The length and diameter of the TPI tubes can be tuned by introducing sonication and by changing the assembly temperature. Investigation of changes in the morphology with time indicated that the TPI nanotubes were obtained by the rolling and seaming of certain preorganized 2D lamellar structures. The results of nuclear magnetic resonance (NMR), X-ray photoelectron spectroscopy (XPS), and absorption spectra revealed that the lamellar structures were constructed through the cooperation of three chemically orthogonal and spatially independent noncovalent intermolecular interactions, namely, hydrogen bonds, $\pi$-$\pi$ interaction, and van der Waals contact. With a similar method of assembly, Zhang and coworkers also prepared tubular structures of an intramolecular charge-transfer compound;[121] Wang and coworkers obtained luminescent nanowires from several quinacridone derivatives;[122] while Zang and coworkers prepared nanofibers and nanobelts from several kinds of small conjugated molecules.[123–125]

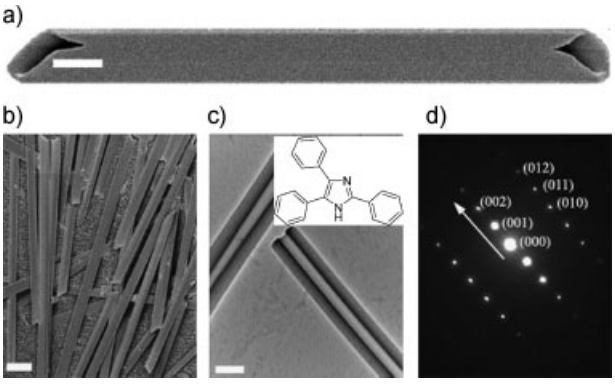


**Figure 3.** a) Typical SEM image of a single TPI nanotube; scale bar represents 200 nm. b) SEM image of the tubes; scale bar represents 500 nm. c) TEM image of the tubes; scale bar represents 200 nm. Inset: Chemical structure of a single TPI molecule. d) SAED pattern of the tubes along the [100] zone axis with the main diffraction spots indexed. (Reprinted from [120]. Copyright 2005 American Chemical Society.)

#### *2.2.2. Self-Assembly Through Organogelation*

A gel denotes a dilute mixture of at least two components, in which each of the components forms a separate continuous phase throughout the system. Generally, gels are divided into two groups, chemical gels and physical gels, depending on the type of interactions that hold the network structure together. The gels formed from low molecular mass organogelators (LMOGs) belong to the physical type, because the network structures are held together by noncovalent interactions such as hydrogen bonding or $\pi$-$\pi$ stacking, and, in addition, solvophobic and entropy effects are also very important in the formation of organogels.

It has been realized that forming organogels is a very effective way to construct organic 1D nanomaterials with a variety of structures and properties.[126–128] Commonly used organogelators include carbohydrate derivatives,[129] amphiphilic molecules,[130] substituted cyclohexane,[131] and cholesterol derivatives.[132] Usually, long alkyl chains or steroidal groups are incorporated into most gelator molecular structures to achieve effective gelation, although these structural elements are normally inactive and undesirable for the optoelectronic properties. Park and coworkers reported a new class of LMOGs, 1-cyano-*trans*-1,2-bis(3′,5′-bistrifluoromethyl-biphenyl)ethylene (CN-TFMBE) with simple $CF_3$ substituents.[133] As displayed in Figure 4, thermoreversible gels were obtained by the gelation of dichloroethane by CN-TFMBE. The SEM images shown in Figure 4c suggest that CN-TFMBE created entangled 3D networks consisting of bundles of fibrous aggregates. Figure 4d indicates that the gelation induced strong fluorescence emission, although CN-TFMBE monomers are totally nonfluorescent in

  

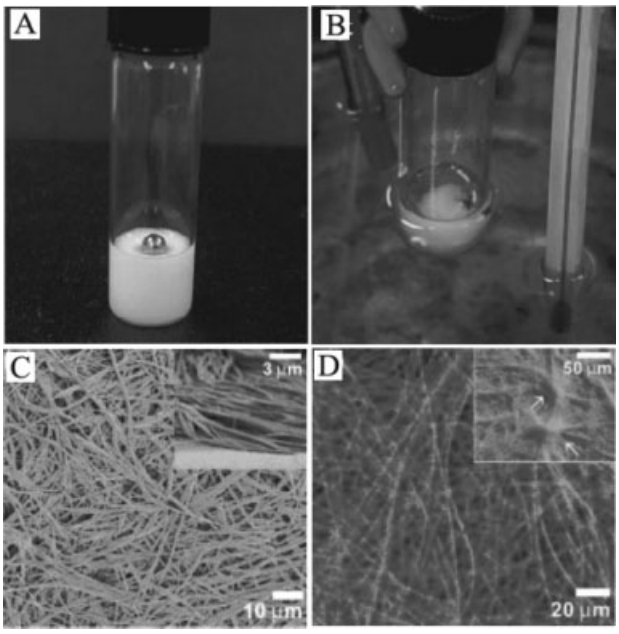


**Figure 4.** a) CN-TFMBE gel sample on which a metal ball is placed at room temperature. b) The same gel sample immersed in a temperature-regulated bath at 51 °C. c) SEM images of a dried CN-TFMBE gel. d) Fluorescence microscopy images of a CN-TFMBE organogel. (Fig. 4c,d reprinted from [133]. Copyright 2004 American Chemical Society.)

1,2-dichloroethane solution. Analogue experiments proved that the unique gelation capability of CN-TFMBE was endowed by the simple $CF_3$ groups through two structural features: 1) the rigid-rod-like aromatic segments exerted strong $\pi$-$\pi$ stacking interactions, and 2) the $CF_3$ components induced and stabilized molecular assembly with its strong secondary bonding forces.

### 2.2.3. Self-Assembly with Solvent Evaporation

Most organic materials dissolved in certain solvents will aggregate and self-assemble when the solvents evaporate. However, the size, morphology, and uniformity of the assembled products are not easy to control, especially in the nanometer regime, although it is possible to achieve well-defined macroscopic single crystals. Recently, Yao and coworkers introduced sonication to the solvent evaporation process and prepared TPI 1D nanomaterials with tunable morphologies.[134] The substrates (glass or quartz) were first suspended in 5 mL TPI solutions with various solvents and concentrations. The solutions were subsequently put into a commercial ultrasonic cleaning bath and sonicated for about 10 min. The solvents evaporated as the sonication proceeded, and the TPI molecules assembled into nanocrystals spontaneously on the surfaces of the substrates. It was found that the concentration of the initial solutions and the sort of solvents influenced the topology of the final products. Nanotubes with rectangular sections were prepared with lower TPI concentration in ethanol, and ordered arrays composed of hundreds of TPI nanorods were obtained when the concentration was increased. Multipods were prepared by changing the solvent to acetone; the concentration of acetone solution hardly affected the final morphology.

### 2.2.4. Template Method: Soft Templates

The template method is a straightforward way to fabricate nanostructures by inducing the target materials to grow according to the patterns of the templates. This strategy provides an easy way for the synthesis of nanomaterials with desired shape and size, and has been widely applied in the construction of 1D nanostructures. The templates adopted in this method can be generally divided into two sorts: soft and hard ones. So-called soft templates are those that can be dissolved in the liquid phase, including surfactant micelles,[135] complexes,[136] biomolecules,[137] and copolymers.[138]

It is well known that micelles (or inverse micelles) with different shapes, such as spherical or rodlike, will be formed in the surfactant solutions when the concentration reaches the critical micelle concentration (CMC).[139] These can then be used as soft templates for the fabrication of nanostructures. Yao and coworkers reported nanofibers of 1,3-diphenyl-2-pyrazoline (DP) induced by CTAB micelles.[140] Figure 5A shows the SEM morphology of the prepared DP nanofibers. It is found that the shape and size of the obtained nanostructures can be controlled by changing the molar ratio of DP to CTAB. Figure 5B illustrates the formation mechanism of the nanofibers. It can be seen that at lower DP/CTAB molar ratios, CTAB tends to form spherical micelles, and increasing the DP/CTAB ratio will

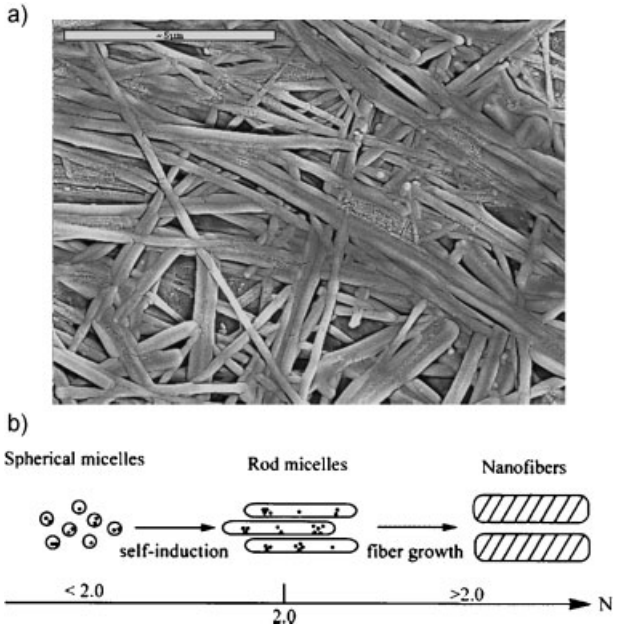


**Figure 5.** a) SEM image of the prepared DP nanofibers; scale bar represents 5 μm. b) Representation of the formation mechanism of the DP nanofiber, in which *N* is the molar ratio DP/CTAB. (Reprinted from [140].)

induce the sphere-to-rod transition of the micelles, which act as a template to direct the 1D growth of DP. With the same method, Wan and coworkers also prepared nanotubes from zinc mesotetra(4-pyridyl)porphyrin and constructed 3D arrays on substrates.[141] Zhang et al. used sodium dodecyl sulfate (SDS) micelles as templates to direct the 1D growth of pyrene molecules in an aqueous phase.[142]

### 2.2.5. Template Method: Hard Templates

The synthesis of nanostructures with hard templates has developed independently in various fields of nanotechnology and it has become one of the most applied methods in the fabrication of inorganic 1D nanomaterials.[70,143] Possin was the first to use this technique to prepare semiconductor nanowires in the 1970s,[144] and Martin extended this technique and first put forward the term ''template synthesis'' in the 1990s.[70,143] Now the commonly used templates include but are not limited to ordered porous membranes prepared with anodized aluminum oxide (AAO),[92] silica,[145] nanochannel glass,[146] and ion-track-etched polymers.[147]

In recent years, this technique has also been applied to prepare 1D nanomaterials from small organic compounds. For example, Lee et al. reported the synthesis of organic nanowires by introducing 1,4-bis[2-(5-phenyloxazolyl)]benzene molecules into the AAO membranes by sublimation.[148] Li and coworkers fabricated $C_{60}$ nanotubes with this method by an easy dip-and-dry procedure, in which they dipped the AAO templates repeatedly into a $C_{60}$ solution, and evaporated the solvent during the intervals between dipping.[149]

Yao's group reported the preparation of perylene[150] and dibenzoylmethane (DBM)[151] nanotubes by the dip-and-dry template method followed by heat treatment to increase the crystallinity. Figure 6a shows a SEM image of DBM nanotubes with 200 nm diameter. DBM nanotubes of different sizes were prepared by using alumina templates with different pore diameters. $\beta$-Diketones, of which DBM is an example, are of interest in different areas owing to their isomeric keto–enol interconversion, as shown in Figure 6b. It is interesting to note that the conversion equilibrium was modulated by altering the size of the tube, that is, the ratio of the enol isomers increased with a decrease of the diameters of the nanotubes.

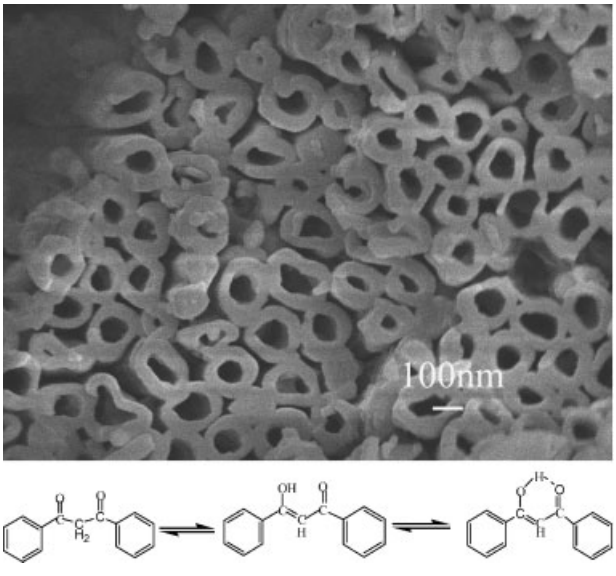


**Figure 6.** a) SEM image (top view) of DBM nanotubes of 200 nm diameter after the complete removal of the AAO templates. b) Equilibrium showing the keto–enol isomerism of DBM molecules. Reprinted from [151].

### 2.2.6. Vapor Deposition

Vapor deposition (VD) is a facile and feasible method for preparing nanomaterials and has achieved great success in fabricating inorganic 1D nanostructures, polymeric thin films, and inorganic–polymer nanocomposites. However, the monodispersity of the products is hard to control when small organic molecules are selected as deposition sources. It is known that for VD the degree of saturation is the predominant factor in controlling the morphology and dispersity of the products,[152] and it should be possible to process most solid materials into 1D nanostructures by maintaining the vapor saturation at a low level. Several techniques have been adopted to control the local supersaturation in the preparation of organic 1D nanomaterials by VD. For example, Lee et al. introduced AAO templates to the VD experiment,[148] Rubahn and coworkers[153] and Perng and coworkers[154] controlled the substrate temperatures to ensure the uniform 1D growth of organic molecules, and Li and coworkers[155] introduced solid-phase reactions into the VD method to control the supersaturation.

So far, most of the achieved organic nanomaterials are amorphous and it will be of great significance to find a general method for the construction of crystalline nanomaterials, because crystals reveal the intrinsic properties of materials more exactly and the crystalline structures of the organic nanomaterials can effectively enhance the performance of the corresponding devices.[156] Recently, Yao and coworkers reported an adsorbent-assisted physical vapor deposition (PVD). Adsorbents such as neutral aluminum oxide or silica gel, used widely in column chromatography, were introduced into the PVD method to control the degree of saturation, considering that there should exist an adsorption–desorption equilibrium between the adsorbents and the organic sources. A series of single-crystalline 1D organic nanostructures were prepared with this method.[157–160] Figures 7A and B show typical SEM and TEM images of tris(8-hydroxyquinoline)aluminum ($Alq_3$) nanowires. The SAED pattern shown in Figure 7C reveals that the $Alq_3$ nanowires are single-crystalline structures with preferential growth along the $[10\bar{1}]$ direction, which is also testified by the XRD patterns. The length and diameter of the nanowires prepared with this method can be well controlled by varying the deposition conditions, such as time and temperature. The results of analogous experiments and thermogravimetric analysis (TGA) measurements displayed in Figure 7D indicate that the addition of adsorbents is indispensable in improving

  

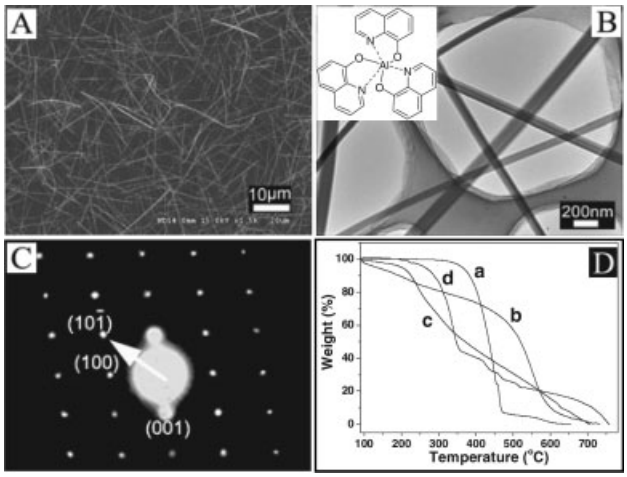


**Figure 7.** A) FE-SEM image of $Alq_3$ nanowires with 300 nm diameter and 20 μm length. B) TEM image of some typical $Alq_3$ nanowires. Inset: Chemical structure of a single TPI molecule. C) SAED pattern of the $Alq_3$ nanowire; the arrow indicates the direction of the wire. D) TGA plots of a) pure $Alq_3$ powder, b) a mixture of $Alq_3$ with aluminum oxide, c) a mixture of $Alq_3$ with silica gel, and d) a mixture of $Alq_3$ with sodium chloride. The weights of $Alq_3$ are normalized as 100% for all the samples. (Reprinted from [157].)

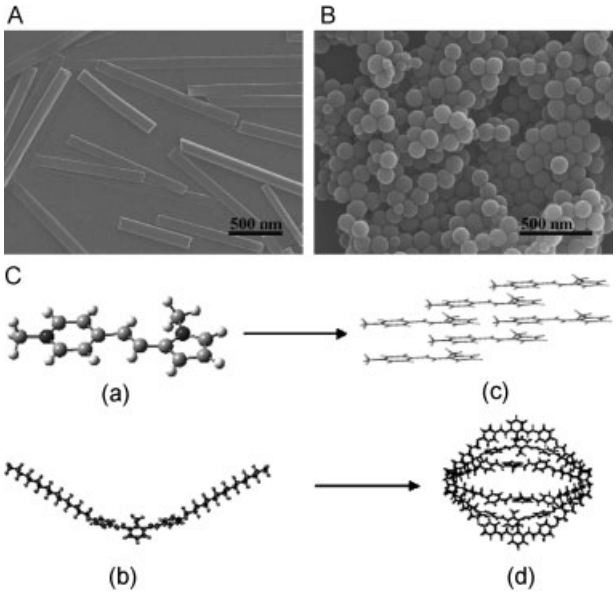


**Figure 8.** A) SEM image of the nanorods formed from **1**. B) SEM image showing a large quantity of the nanospheres prepared with **2**. C) Schematic illustration of the aggregation modes of target compounds, in which (a) and (b) are optimized structures of **1** and **2** single molecules, respectively; (c) and (d) are the simulated 1D and 0D aggregation of **1** and **2**, respectively. (Reprinted from [163].)

the uniformity of the nanowires. It can be observed that the adsorbents decreased the sublimation temperature and slowed the weight loss of $Alq_3$ remarkably, through which the degree of saturation and the uniformity can be readily controlled. In contrast, the introduction of sodium chloride, which does not adsorb, hardly affects the slope of the TGA plot. No catalyst was used and no droplet was found at the top, so the growth of the 1D materials prepared with this method should be controlled by the vapor–solid (VS) process.[152] The unique luminescent properties of the 1D nanomaterials achieved with this strategy will be discussed in Section 3.

### 2.3. Morphology Control Between 0D and 1D

Controllable synthesis is a key task for nanoscale science, and the morphologies of inorganic nanostructures have been successfully controlled by choosing appropriate materials and changing the synthesis methods.[161,162] However, the morphology control of organic nanomaterials has met with limited success. The commonly used strategy to modulate the organic nanostructures is to slightly alter the molecular structures in a series of derivatives. For example, Zang and coworkers have prepared either nanobelts or nanospheres by using two different derivatives of perylene diimide.[123,124] Recently, Yao's group has tried several means for this purpose, which are illustrated in the following two sections.

#### *2.3.1. Self-Assembly of Dyes with Different Substituents*

The facile fabrication of nanostructures with well-defined shapes and uniform sizes from stilbazolium-like dyes was reported.[163] Stilbazolium-like dyes **1** and **2** (Fig. 8) with different substituents (Fig. 8) were synthesized with the intention of exploring the possible influence of the substituent on the shape and therefore the optical properties of the resulting nanostructures. The self-assembly of the target molecules was induced by solvent exchange. Figures 8A and B display SEM images of compounds **1** and **2**, respectively, assembled in nonsolvents. It can be seen that changing the substituents influenced the morphology of the aggregates significantly.

As shown in Figure 8C, molecule **1** consists of a strong electron-withdrawing moiety *N*-methylpyridinium (Nmpd) and a strong electron releasing group *N*-methylpyrrole (Nmpr) connected by a conjugated system. For molecule **2**, two weaker electron-releasing groups, 4-hexadecyloxyphenyl (4Hop), are connected to the Nmpd moiety. In addition, **1** is a planar molecule, so strong donor–acceptor interactions are the main driving force for the aggregation of **1** and induce the formation of 1D nanostructures.[164] In comparison, **2** is a nonplanar molecule with weak donor–acceptor interactions. There are two long flexible alkyl side chains on the ionized pyridine ring, and therefore **2** is a typical amphiphilic molecule bearing a hydrophilic head (ionized pyridine ring) and two long and flexible hydrophobic arms (alkyl chains), which will drive the molecules to form H-aggregates with monodisperse spherical morphologies as shown in Figure 8C.

#### *2.3.2. Other Self-Assembly-Based Methods*

Besides nanostructures made from compounds with different substituents, nanostructures with well-defined shapes, such as spheres, square wires, and cubes, have also been prepared by

the self-assembly of three isomeric molecules of bis(iminopyrrole)benzene with the same substituents at different positions.[165] Although all three isomeric precursors, *o*-, *m*-, and *p*-bis(iminopyrrole) benzene, exhibit similar, strong, multiple hydrogen-bonding interactions for molecular aggregation, distinctly shaped nanostructures were obtained. The two iminopyrrole (IP) groups in the *o*-isomer are 60° open-armed. Therefore, two monomers can interlock to form a dimer by means of quadruple hydrogen bonds, which act as the basic units for the formation of spherical structures. In contrast, the configurations of *m*- and *p*-isomers, with two IP groups open-armed at angles of 120° and 180°, respectively, determine that each molecule connects with two other molecules with hydrogen bonds, forming chain-like structures. Also determined by the molecular configurations, the chain of the *m*-isomer is zigzag shaped while that of the *p*-isomer is almost linear. These chains are the building blocks for the solid states of the two isomers to form square wires and cubes, respectively. It is the different interactions for aggregate stacking at supramolecular level caused by the isomeric molecular structures that are responsible for the different morphological evolution.

Another method to control the dimension is to induce the self-assembly of organic molecules on the surface of nanostructures with different morphologies.[166] First, 0D copper nanoparticles and 1D nanorods were fabricated selectively through the reduction of $CuSO_4$ in aqueous solutions. The only difference between the synthesis parameters of copper nanorods and those of copper nanoparticles lies in the introduction of poly(*N*-vinyl pyrrolidin-2-one) (PVP), which is widely used in the synthesis of 1D nanomaterials because the growth rate of different crystal planes can be kinetically controlled by the interaction of PVP with these planes by adsorption and desorption.[167] Subsequently, TPI molecules were induced to self-assemble hierarchically into higher-order structures at the surfaces of 0D and 1D copper nanostructures, respectively. The copper nanostructures provided a template for the growth of TPI, and the size and morphology of the TPI nanostructures were readily controlled by just altering the morphology of the copper cores. It is interesting to note that the optical properties of the TPI shell materials can be tuned by just changing the size of the inner nanometer-scale copper.

### 2.4. Beyond 0D and 1D Structures

Besides 0D and 1D nanomaterials, there have also been some reports on other organic nanostructures, that is, hierarchical assemblies of simple nanoscale building blocks. The integration of relatively simple building blocks into mesoscopic higher-order architectures with complex form and hierarchy is characteristic of biological systems and has been investigated extensively in the inorganic area,[168] because it is known that the properties of the mesoscopic assemblies differ from those of the isolated nanocrystals as well as those of the bulk phases.

During the past several years, the unique optoelectronic properties have also sparked widespread investigation of hierarchical self-assembly of organic building blocks achieved by the induction of noncovalent intermolecular interactions, for instance, hydrogen bonding, $\pi$-$\pi$ stacking, van der Waals forces, coordination interaction, etc. For example, Yao and coworkers reported novel peony-like and actinia-like mesostructures based on a stilbazolium-like dye induced by using specific poor solvents.[169] Characterization with a combination of correlation spectroscopy (COSY) and 2D nuclear Overhauser enhancement spectroscopy (NOESY) techniques suggested that multistage association was responsible for the formation of the ordered mesostructures. They further induced 4,5-diphenylimidazole (DPI) to self-assemble hierarchically into higher-order mesostructures at the copper–solution interface by utilizing the coordination interaction between DPI and copper.[170] The DPI–copper complexes played a decisive role in the formation of DPI mesostructures. By changing the assembly conditions, superstructures with different morphologies were obtained. The DPI mesostructures are superhydrophobic and can inhibit the corrosion of copper significantly. With a similar technique, Hu and coworkers also prepared assemblies of Cu-TCNQ on copper surfaces, where TCNQ is tetracyanoquinodimethane.[171]

## 3. Optoelectronic Properties

Besides the exploration of the synthetic strategies, much effort has also been made to investigate the unique optical and/or electronic properties of the organic nanomaterials obtained by molecular aggregation in the nanostructures. As mentioned above, it was found that the optical and electronic properties of organic nanomaterials are fundamentally different from those of their inorganic counterparts, because the intermolecular interactions in organic materials are basically of weak types, such as hydrogen bonds, $\pi$-$\pi$ stacking, van der Waals contacts, and CT interactions. In this section, we give an overview of current studies on the optoelectronic performance of organic nanostructures. First, the size-dependent optical properties are discussed, then more attention will be paid to the unique photoluminescent properties, and finally the electric and electronic properties are also introduced briefly.

### 3.1. Size-Dependent Optical Properties

The size-dependent optical properties of organic nanoparticles, which are similar to but cannot be explained by the so-called quantum confinement effect observed in inorganic semiconductor quantum dots, were first observed in perylene nanocrystals and reported by Nakanishi and coworkers.[172] In addition, Horn and coworkers investigated the effect of both supramolecular structure and particle size on the absorption spectra of $\beta$-carotene nanoparticles.[106] Recently, Yao's group

  

also systematically investigated the size-tunable optical properties of organic nanoparticles prepared from a series of aromatically substituted pyrazoline compounds. In the following four sections, we will outline the effect of size on the absorption and luminescence properties of these nanoparticles based on pyrazoline compounds.

### 3.1.1. Exciton Confinement Effect

Nanoparticles were prepared from 1-phenyl-3-((dimethylamino)-styryl)-5-((dimethylamino)phenyl)-2-pyrazoline (PDDP) by reprecipitation.[173] Figure 9 shows the absorption spectra of the PDDP nanoparticles and PDDP monomers in ethanol. In solution, there are three resolved absorption bands arising from the phenyl ring transition and the pyrazoline ring n-$\pi^*$ and $\pi$-$\pi^*$ transitions, labeled $P_{phenyl}$, $P_{n\text{-}\pi^*}$ and $P_{\pi\text{-}\pi^*}$, respectively. All three bands did not shift when the concentration of the solution changed from $1.0 \times 10^{-5}$ to $1.0 \times 10^{-3}$ mol $L^{-1}$. For the nanoparticles, when the size increased from tens to hundreds of nanometers, the $P_{phenyl}$ and $P_{\pi\text{-}\pi^*}$ bands were observed to shift to longer wavelength, and concomitantly a new peak gradually appeared and also shifted to the lower energy side. This bathochromic shift was proposed to result from the increased overlap of the pyrazoline ring $\pi$-orbital and intermolecular interactions between PDDP molecules when the nanoparticle size increased. The newly emerged absorption peak ($P_{CT}$) was ascribed to the transition from an extended charge-transfer (CT) state of PDDP aggregates derived from PDDP molecules closely stacked in the nanoparticles. The red shift was considered to result from the CT exciton confinement effect.

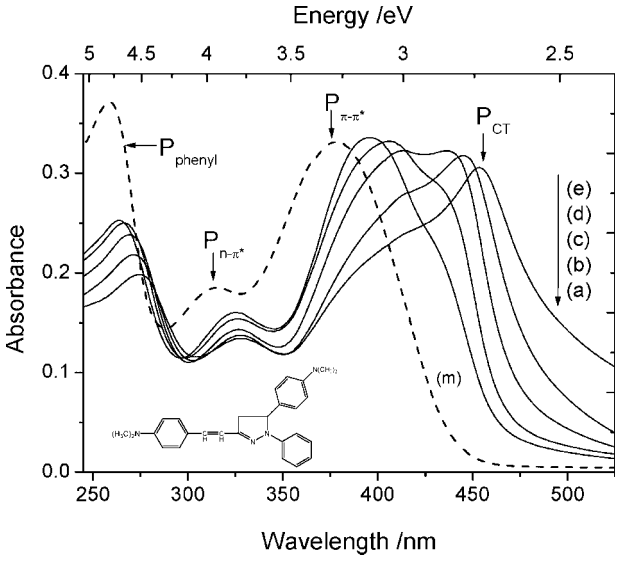


**Figure 9.** UV-vis absorption spectra of PDDP nanoparticle dispersions in water with different sizes: a) 20 nm, b) 50 nm, c) 105 nm, d) 190 nm, and e) 310 nm. Curve m: The spectrum of the PDDP/ethanol solution ($1.0 \times 10^{-5}$ mol/L). Inset: The molecular structure of PDDP. (Reprinted from [173]. Copyright 2001 American Chemical Society.)

### 3.1.2. Size-Tunable Emission

Organic nanoparticles with average diameters ranging from 40 to 160 nm were prepared from another pyrazoline compound, 1,3-diphenyl-5-(2-anthryl)-2-pyrazoline (DAP).[174] It was found that the absorption transitions of the DAP nanoparticles at the lower-energy side experienced a bathochromic shift with an increase of the particle size as a result of increased intermolecular interactions, while the higher-energy bands of anthracene split due to the electronic coupling between the pyrazoline ring of one molecule and the anthracene moiety of the neighboring one. It is worth noting from Figure 10 that the nanoparticle emission in the blue light region from the pyrazoline chromophore shifted to shorter wavelengths with an increase in particle size, accompanied by a relatively gradual dominance of the emission at about 540 nm from the exciplex formed by the pyrazoline ring of one molecule and the anthracene moiety of the neighboring molecule. The hypsochromic shift in the emission of DAP nanoparticles was identified as originating from the pronounced decrease in the Stokes shift due to the restraint of vibronic relaxation and the configuration reorganization induced by increased intermolecular interaction.

### 3.1.3. Multiple Emissions

In the case of 1,3-diphenyl-5-pyrenyl-2-pyrazoline (DPP),[175] the nanoparticles showed different emission behavior compared to either the solution or the bulk material. DPP contains two chromophores, the pyrene and pyrazoline groups, whose conjugated systems are separate from each other due to the steric effect. Dilute solutions exhibit only the emission characteristics of the pyrene chromophore, while the bulk material shows only the emission of the pyrazoline chromophore.[176] However, the nanoparticles presented multiple emissions from

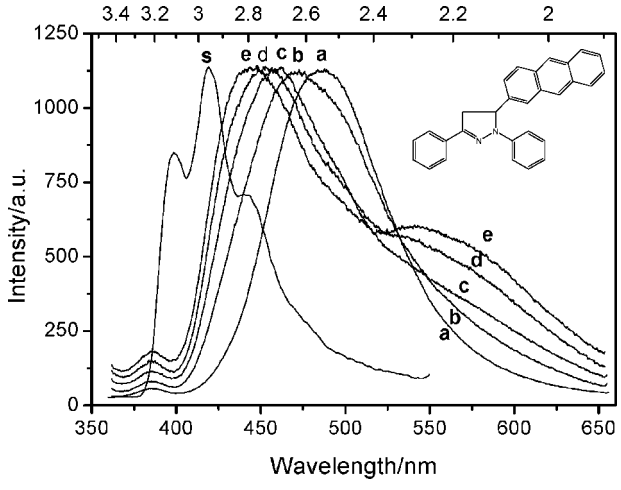


**Figure 10.** Fluorescence emission spectra of DAP nanoparticle dispersions with different sizes: Curve a) 40 nm, b) 60 nm, c) 90 nm, d) 120 nm, e) 160 nm. Curve s: The spectrum of DAP solution in acetonitrile. The excitation wavelength for all the samples is 350 nm. Inset: The molecular structure of DAP. (Reprinted from [174]. Copyright 2003 American Chemical Society.)

ADVANCED MATERIALS



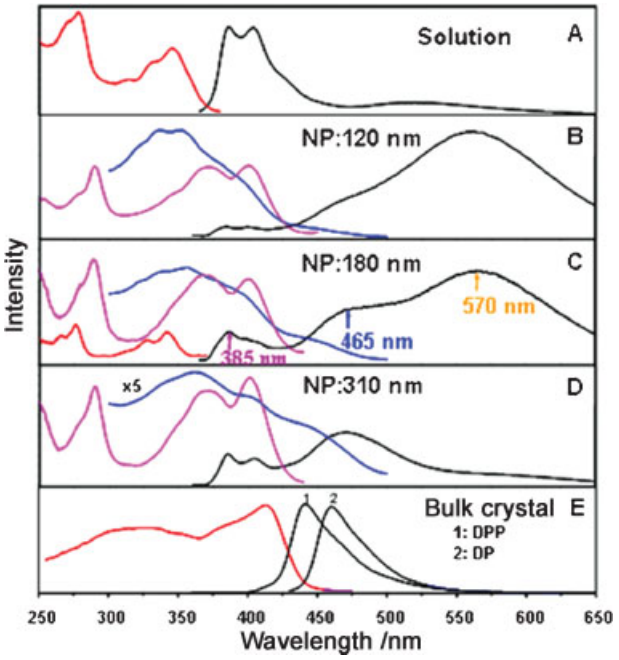


**Figure 11.** The fluorescence excitation and emission spectra of A) DPP solution (in acetonitrile, $1.0 \times 10^{-5}$ mol $L^{-1}$), B–D) DPP nanoparticles (NPs) with different sizes, and E) DPP and DP bulk crystals. The colored lines are the excitation spectra obtained by monitoring the emission at 385 (red), 465 (purple), and 570 nm (blue), except for the red line in (E), which was obtained by monitoring the emission of DPP at 445 nm. Black lines are emission spectra obtained by excitation at 345 nm. (Reprinted from [175].)

pyrene, pyrazoline, and additionally a CT complex between pyrene and pyrazoline. As shown in Figure 11, the relative intensity of the emissions was dependent on the size of the nanoparticles. Moreover, these emissions possess an individual optical channel and can be excited by their original excitation wavelength, which means that the emission can be tuned by alteration of either the excitation wavelength or the particle size. The multiple emissions and their evolution as a function of particle size were considered to be caused by molecular aggregation and surface effects.

#### *3.1.4. Other Size-Dependent Properties*

Besides the above mentioned size-tunable optical properties, Yao and coworkers also investigated size-dependent exciton chirality in organic nanoparticles.[177] They prepared nanoparticles from a chiral auxiliary, (*R*)-(+)-1,1′-bi-2-naphthol dimethyl ether (BNDE), with a range of particle sizes from 25 to 100 nm. The BNDE nanoparticles exhibited positive exciton chirality in the 200–260 nm region in circular dichroism (CD) spectra, which is completely opposite to CD spectra of the dilute solution. The exciton chirality peaks evolved to the low-energy side with an increase in particle size. The chirality inversion resulted from intermolecular exciton coupling between two adjacent BNDE molecules in the nanoparticles, and the bathochromic shift of the peaks was attributed to increased intermolecular interaction with increasing particle size. They also prepared nanoparticles from an azo transition metal chelate compound and investigated the third-order nonlinear optical (NLO) properties.[178] The enhanced and size-tunable off-resonant third-order NLO responses of these nanoparticles were confirmed. The NLO enhancement of the nanoparticles compared to that of the monomer was proved to originate from the increased intramolecular CT process due to the improved planarity of the ligands. The size-dependent NLO responses of the nanoparticles were attributed to the gradual predominance of the intermolecular CT at the expense of the intramolecular CT with increasing particle size.

### 3.2. Unique Photoluminescent Behaviors

The quantum confinement effect introduces many novel photoluminescent (PL) properties to inorganic nanomaterials. For organic nanomaterials, although so-called quantum confinement has not been observed, a series of unique PL behaviors has been achieved, which resulted from the special aggregation modes of the organic molecules, the crystallinity of the materials, and the deliberate introduction of at least one kind of guest compound into the host material matrices. In the following sections, we introduce the particular PL properties of organic nanomaterials, including emission enhancement in amorphous nanostructures, fluorescence narrowing and defect emission from organic crystalline nanomaterials, and tunable and switchable emissions from doped organic nanosystems.

#### *3.2.1. Aggregation-Induced Enhanced Emission*

In general, the fluorescence efficiency of organic chromophores decreases in the solid state, as a result of concentration quenching, even though they show high fluorescence efficiency in solution. However, a phenomenon named aggregation induced enhanced emission (AIEE) was reported in recent years, in which enhanced emission instead of fluorescence quenching was observed in the solid state for some fluorophores.[179,180] These findings provide a possible solution to the limitation caused by concentration quenching in applications such as ultrahigh density optical memory and full color flat panel displays.

Recently, Park and coworkers reported AIEE from organic nanoparticle systems.[181] They synthesized the organic molecule 1-cyano-*trans*-1,2-bis-(4′-methylbiphenyl)ethylene (CN-MBE) and prepared the corresponding nanoparticles. It is interesting to note that although the fluorescent emission from CN-MBE solution was very weak, the nanoparticles emitted a very strong photoluminescence with intensity almost 700 times that of the solution (Fig. 12A). It was proposed that the aggregation induced the planarization of the CN-MBE molecules in the nanoparticles, which in turn resulted in the strong intermolecular interactions causing a specific aggregation. In addition, the bulky and polar cyano group restricted the parallel face-to-face intermolecular interactions and prevented parallel orientation of conjugated chromophores, which favored the formation of *J*- instead of *H*-aggregation and restricted excimer

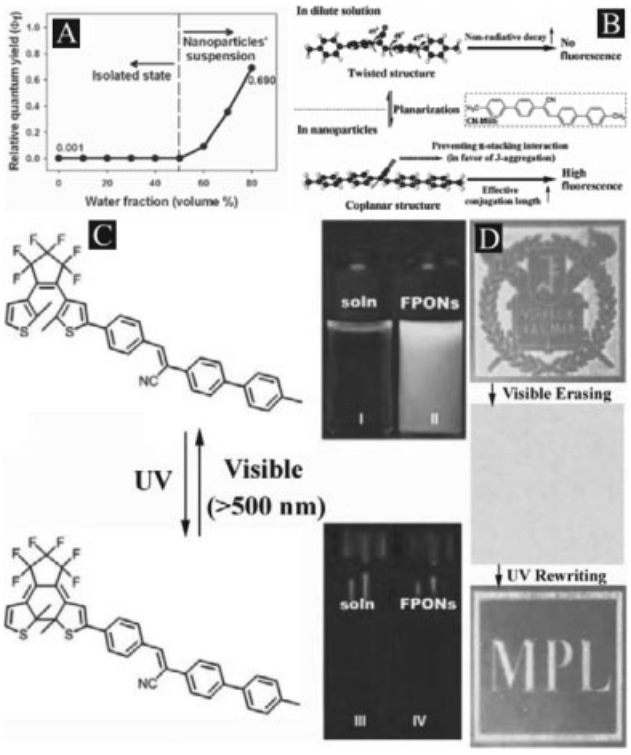


**Figure 12.** a) Relative quantum yields of CN-MBE ($2 \times 10^{-5}$ mol $L^{-1}$) depending on water fractions in THF. The addition of water induces the aggregation of CN-MBE molecules. b) Proposed mechanism of enhanced emission in CN-MBE nanoparticles. Inset: The molecular structure of CN-MBE. (Reprinted from [181]. Copyright 2002 American Chemical Society.) c) Chemical structures and fluorescence images of the open-ring (top) and closed-ring (bottom) BTE-CN-MBE. d) Photo-rewritable fluorescence imaging on the polymer film loaded with 20 wt% of BTE-CN-MBE nanoparticles using UV (365 nm, hand-held lamp, 1.2 mW $cm^{-2}$) and visible light (>500 nm). The dark regions represent the parts irradiated with UV light; the real size of the photomasks is about 1 cm × 1 cm. (Reprinted from [182].)

formation in the solid state (Fig. 12B). The synergetic effect of intramolecular planarization and *J*-aggregate formation in the nanoparticles was considered to be responsible for the enhanced emission.

On the basis of this work, Park and coworkers also designed a multifunctional fluorescent molecule for photoswitchable memory media by replacing one of the end tolyl groups in CN-MBE with the photochromic 1,2-bisthienylethene (BTE) moiety.[182] As shown in Figure 12C, this compound provided an opportunity to combine the AIEE property of the CN-MBE unit with the bistable photochromism of the BTE unit to solve the general problem of concentration quenching in the fluorescence switch system. With this novel compound, they prepared size-controllable nanoparticles. They further used the neat nanoparticles and a nanoparticle-loaded poly(methyl methacrylate) (PMMA) film as photoswitchable memory media, with which they achieved information storage with high capability, high sensitivity, and high-contrast on/off signal ratio. Figure 12D illustrates photo-rewritable fluorescence imaging on the polymer film loaded with 20 wt% of BTE-CN-MBE nanoparticles.

### *3.2.2. Unique Luminescence from Crystalline 1D Organic Nanomaterials*

Most of the organic nanomaterials prepared so far are amorphous in structure. It was mentioned in Section 2 that Yao's group has developed an adsorbent-assisted PVD strategy for the general construction of crystalline 1D organic nanostructures.[157–160] It was revealed that the crystallinity of the nanomaterials resulted in some novel luminescent behaviors. In this section, we introduce the fluorescence narrowing and multicolor emission from crystalline nanowires and nanoribbon arrays, respectively, based on a single chemical composition prepared by this method.

*Fluorescence Narrowing*: First, the single-crystalline nanowires were fabricated from a small organic functional molecule, TPI (see Fig. 3 for the chemical structure), by adsorbent-assisted PVD,[158] in which the introduction of the adsorbents proved to be indispensable for improving the uniformity of the TPI nanowires. The SAED and XRD results indicate that the TPI nanowires are single crystalline and grow along the *b*-axis of the TPI crystal. Moreover, the degree of preferential orientation was obviously strengthened with the decrease of diameter from 500 nm to 40 nm.

The optical properties of the TPI nanowires are primarily dependent on the diameter and insensitive to the length. Figure 13 displays the fluorescence emission spectra of TPI nanowires with different diameters. The spectrum of the TPI monomer measured at ambient temperature shows an approximately symmetric peak centered at 383 nm, whereas the vibronic levels are well resolved in the low-temperature spectrum measured at 77 K. It is interesting to note that the

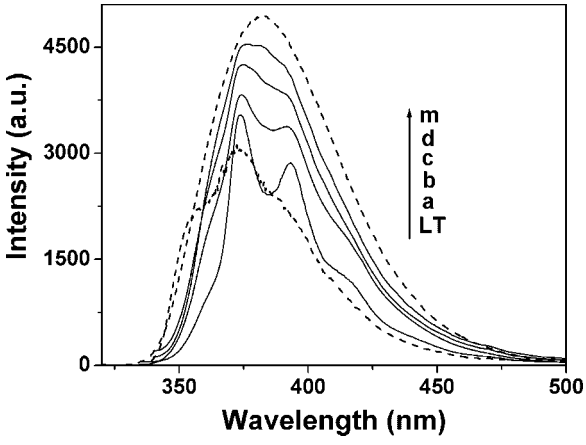


**Figure 13.** Fluorescence emission spectra of TPI nanowires with different diameters deposited onto quartz wafers: a) 40 nm, b) 120 nm, c) 300 nm, d) 500 nm. Curve m: The spectrum of TPI monomers measured at room temperature. Curve LT: Low-temperature (77 K) fluorescence spectrum of the TPI monomer. All the emission spectra were excited at 310 nm. (Reprinted from [158]. Copyright 2006 American Chemical Society.)

ADVANCED MATERIALS



narrowing of the spectra was also observed in the nanowire samples even at room temperature and became more pronounced with decreasing diameter.

In an amorphous environment, the emission band broadening results mainly from the fact that the molecules each have somewhat different energy levels. In the single-crystalline nanowires, however, the molecules are confined distinctly in the lattice with specific geometric configuration and high degree of orientation. In this case, many molecules share the same energy level, so the degree of freedom of their vibrations is drastically reduced.[183] The local environment of the molecules in the nanowires does not change in time during the emission process, and only those molecules that have energy levels corresponding to the excitation wavelength can be excited, which results in the emergence of the vibrational fine structure. Moreover, the vibrational structure became more and more resolved as the diameter decreased from 500 nm to 40 nm, which was assigned to the increase of long-range order[184] and degree of orientation[185] with decreasing wire diameter.

*Multicolor Emission*: Multicolor emissions, especially red-green-blue (RGB) emissions are essential for displays and flat screens.[186,187] Generally, multicolor emissions are realized with blends of dyes or polymers emitting red, green, and blue light. In very recent work, Yao and coworkers demonstrated that it is also possible to obtain multicolor emission from crystalline 1D nanomaterials and their hierarchical assemblies based on a single low-molecular-weight organic compound.[159] The selected model compound, 1,2,3,4,5-pentaphenyl-1,3-cyclopentadiene (PPCP, inset of Fig. 14a), is a well-known blue-light-emitting dye used as the emitting layer material in electroluminescence devices.[188] After being fabricated to crystalline nanoribbon assemblies, PPCP displayed a multicolor emission property, that is, blue, green, and red emission was achieved by exciting the same sample with appropriate wavelengths.

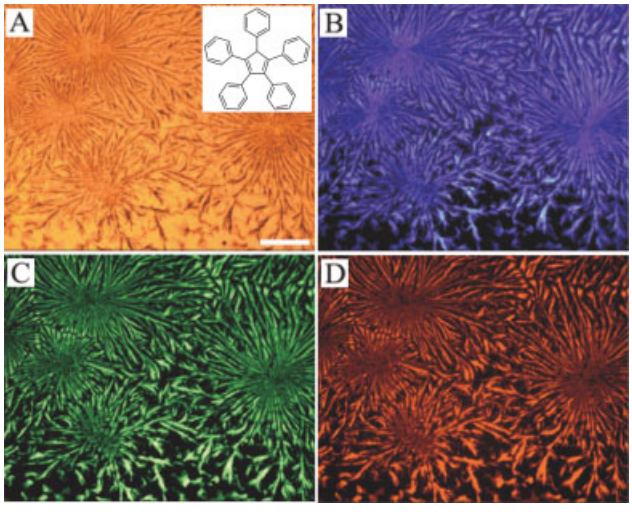


**Figure 14.** Fluorescence microscopy images of the PPCP nanoribbon assemblies. a) Bright-field image. Inset: Molecular structure of PPCP. b) Excited with UV light (330–380 nm). c) Excited with blue light (460–490 nm). d) Excited with green light (520–550 nm). Scale bar represents 10 μm. (Reprinted from [159].)

Figure 14 displays the RGB emission obtained by exciting the PPCP nanoribbon arrays with UV, blue, and green light. The spectral measurements indicated that three kinds of emitting centers (blue, green, and red) coexist in the PPCP nanostructures, in which the blue-light-emitting centers came from the single PPCP molecules in the nanostructures. Comparison of emissions from crystalline nanoribbons with different amounts of defects and the contrast between the emissions from crystalline and amorphous films proved that the green- and red-light-emitting centers in the PPCP nanoribbons were induced by their crystallinity and the structural defect energy levels[189,190] therein. Meanwhile, the emission from each center can be further enhanced by the 1D structure of the nanomaterials by self-convergence along specific directions.

### *3.2.3. Tunable and Switchable Emissions from Doped Organic Nanomaterials*

Doping based on fluorescence resonance energy transfer has been widely used in electroluminescent (EL) devices because it can help to improve the luminescence efficiency and to tune the emission colors.[191,192] In a doped system, the slight variation of the content of energy acceptor will result in significant PL color change. For example, white-light emission, which is pivotal to full-color displays and the backlight of portable display devices, can be obtained by doping blue fluorescent dyes with green and red ones. In addition, the energy transfer also significantly increases the PL quantum yield of the energy acceptor. For instance, the quantum yield of pure rubrene (5,6,11,12-tetraphenylnaphthacene) thin film prepared by vacuum deposition is about 30%, while in films with rubrene as the acceptor the quantum yield can be as high as 100%.[193] Up to now, most organic doping systems are based on amorphous film materials, whereas doped organic nanomaterials, especially crystalline ones, have been paid much less attention. Recently, Yao and coworkers prepared doped organic nanoparticles and crystalline binary organic nanowires, investigated their tunable and switchable emissions, and studied the energy transfer in the doped nanostructures.

*Tunable Emission from Doped Nanoparticles*: First, doped organic nanoparticles were prepared using reprecipitation, with 4-(dicyanomethylene)-2-methyl-6-(*p*-dimethyl-aminostyryl)-4*H*-pyran (DCM, inset of Fig. 15) as energy acceptor and 1,3,5-triphenyl-2-pyrazoline (TPP, inset of Fig. 15) as energy donor.[194] For the preparation, a mixed solution of TPP with DCM was used in the reprecipitation process. As shown in Figure 15, the emission colors of the doped nanoparticles dispersions evolved from blue to red with increasing DCM concentration. The effective quenching of the emission from TPP indicated the occurrence of efficient energy transfer in the nanoparticles. The fluorescence decay measurements proved that the nonradiative Förster resonance type was the dominant mechanism of energy transfer. To fulfill the requirements of practical applications, polymer films dispersed with DCM-

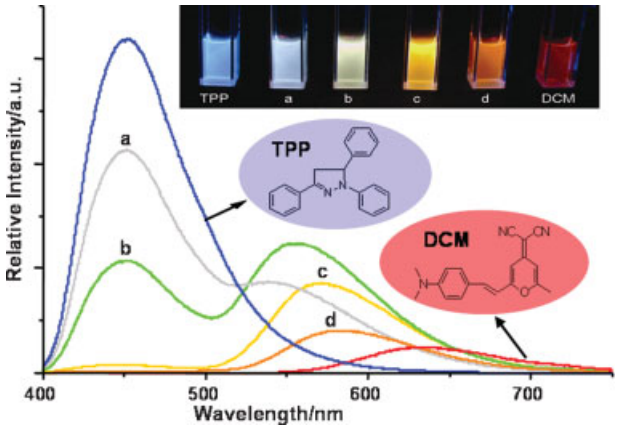


**Figure 15.** Fluorescence emission spectra of suspensions of DCM-doped TPP nanoparticles (intensity of the emission of the dispersion of pure DCM nanoparticles is multiplied by 10 and the excitation wavelength is 365 nm). Inset: Photographs of the fluorescence emissions from suspensions of the doped TPP nanoparticles taken under the UV lamp (365 nm). From left to right, the doping concentrations of DCM are 0, 0.1%, 0.2%, 2%, 10%, and 100% (molar ratio). (Reprinted from [194].)

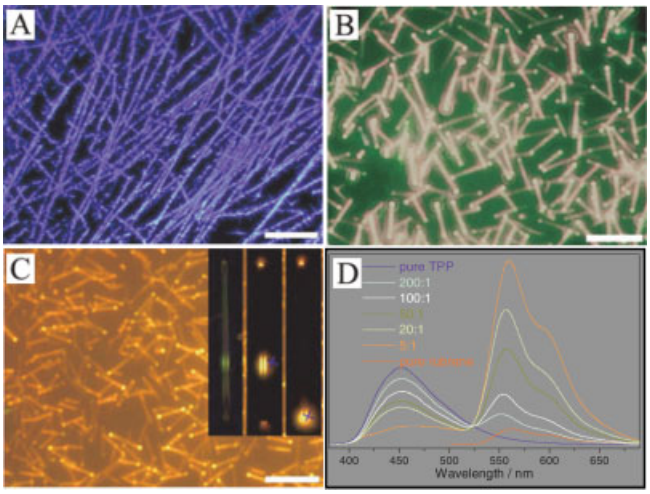


**Figure 16.** a–c) Fluorescence microscopy images of the nanostructures with different rubrene contents. All scale bars represent 5 μm. a) Pure TPP, excited with UV (330–385 nm). b) 100:1 TPP/rubrene, excited with UV. c) Pure rubrene, excited with blue light (460–490 nm). Insets: Bright-field image (left) and micro-area fluorescence images of a single nanorod obtained by exciting the middle part (middle) and top area (right), respectively, using focused laser light. The blue crosses indicate the excited position. d) Emission spectra of the nanowires deposited onto quartz wafers with different TPP/rubrene molar ratios. (Reprinted from [160].)

doped TPP nanoparticles were fabricated, which also demonstrated tunable emissions. Recently Sun et al. also studied this DCM/TPP-doped system theoretically.[195] According to their results, intermolecular charge transfer processes may also be involved in the fluorescence quenching mechanism.

*Tunable Emission from Binary Nanowires*: As mentioned above, an adsorbent-assisted PVD method was developed by Yao and coworkers for the preparation of crystalline 1D organic nanomaterials. In very recent work, they extended this method to binary doped systems. TPP and rubrene were chosen as the model compounds, which were fabricated into uniformly doped crystalline nanorods and nanowires by adsorbent-assisted PVD.[160] The doping content was tuned by changing the molar ratio of the two sources.

Figures 16a–c show fluorescence microscopy images of the binary nanostructures with various doping contents. The homogeneous emission color from all of the nanorods/wires in each sample testified that the rubrene crystal grains were dispersed uniformly in the TPP matrices. It is interesting that there is a bright luminescent point (outcoupling light)[117] at the top of each rod. The characterization by micro-area fluorescence microscopy of single nanorods (insets of Fig. 16c) suggested that the bright points were induced by the optical waveguiding property of the 1D nanostructures. In general, the light emission can only be observed in the vicinity of the excitation position in micro-area fluorescence images. However, for the binary nanorods, the excitation light can propagate to the tops along the length of the rods, irrespective of the excitation position. It is revealed by the fluorescence microscopy images that the emission color evolves from blue to orange with increasing rubrene content and, more interestingly, white emission can be achieved when the proper TPP/rubrene molar ratio (100:1) is used. The tunable emission can also be observed from the evolution of the fluorescence spectra of the nanostructures with change of rubrene content shown in Figure 16d.

For comparison, doped amorphous thin films were also prepared by coevaporation.[196] The colors of the doped films are not stable because of the oxidation of rubrene. In contrast, the emission colors of the binary nanowires are very stable, which was ascribed to the crystallinity of rubrene.[197,198] In the amorphous films, the emission of TPP can be quenched almost completely at 4% rubrene doping content, which is caused by the higher energy transfer efficiency. In contrast, the emission of TPP cannot be quenched completely even when the dopant content is as high as 20% in the doped nanowires. Both the color stability and the incomplete quenching are essential to the realization of white-light emission.

*Switchable Emission in Organic Nanocomposites*: Photoswitches based on photochromic materials have attracted a great deal of interest in recent years because of their potential application as ultrahigh-density optical memory media.[199,200] In most switch systems, the fluorescent probe moieties are covalently bound to the photochromic ones, which can change between two distinct isomeric states, representing 0 and 1 of a digital mode, when irradiated at different wavelengths. The design and synthesis of these multifunctional fluorescent photochromic molecules is a difficult task, especially considering the tunability of the productive absorption bands corresponding to the 'write', 'erase', and 'read' processes.[201]

In recent work, Yao and coworkers described a versatile and convenient approach to achieving fluorescence modulation by

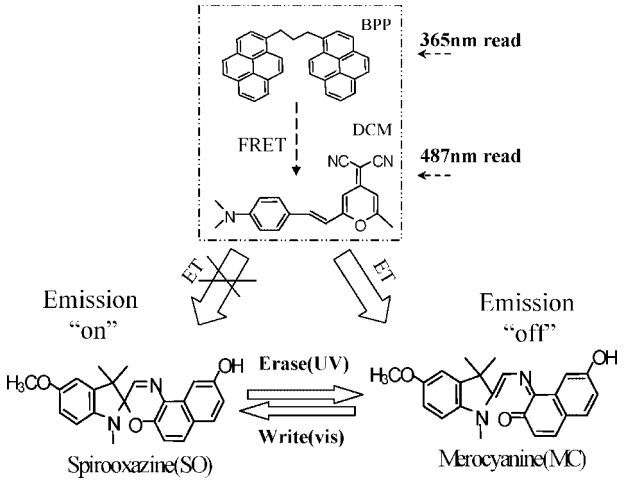


**Figure 17.** Mechanism of fluorescence switching in the doped nanocomposites. FRET: Fluorescence resonance energy transfer. (Reprinted from [202]. Copyright 2007 IOP Publishing.)

the preparation of composite nanoparticles, based on a derivative of photochromic spirooxazines (SO), a typical fluorescent dye DCM, and an emissive assistant molecule of 1,3-bis(pyrene) propane (BPP, see Fig. 17 for the chemical structures), employing doping techniques.[202] It is well-known that there is a photoisomerization between the closed-ring form spirooxazine (SO) and the open-ring form merocyanine (MC), SO ↔ MC, as shown in Figure 17. When the composite nanoparticles were irradiated with UV light, some of the SO isomerized to the MC form, which quenched the emission of DCM via an intermolecular energy transfer. When MC reverted to SO, induced by visible light irradiation, the DCM fluorescence in the nanoparticles recovered fully. The doping of BPP not only enhanced the contrast between the fluorescence ON and OFF signals, but also provided a way to tune the excitation wavelength for reading the fluorescence signals. Figure 17 illustrates the mechanism of the fluorescence switch.

### 3.3. Other Optoelectronic Properties

In addition to the above mentioned luminescent properties, some other optoelectronic properties of organic nanomaterials have also been reported in the past few years. For example, Jalili and Rafii-Tabar investigated the electronic conductance through organic nanowires;[203] Wang and coworkers[154] and Li and coworkers[204] investigated the field emission properties of $Alq_3$ nanowires and TCNQ charge transfer complexes nanowires, respectively. Recently, Hu and coworkers[205] as well as Geohegan and coworkers[206] fabricated field-effect transistors (FETs) based on single-crystalline organic 1D nanomaterials, while Rubahn's group[153,207] and Takazawa's group[117,118,208] reported the optical waveguiding properties of organic nanowires. Lasers have proved to be another promising application for organic 1D nanomaterials.[64,209]

## 4. Summary and Outlook

In this article, we have presented a review of recent research on nanomaterials based on small organic functional molecules. We first introduced the strategies for the construction of organic nanostructures. After an overview of the preparation of 0D organic nanomaterials, we placed more emphasis on the construction of 1D organic nanostructures. The morphology control of organic nanomaterials by means of molecular design and synthesis was also highlighted in that part. In the following section, we reviewed the unique optical and electronic properties of some representatives of the organic nanomaterials prepared to date. In this section, we first introduced the size-dependent optical properties of several kinds of organic nanoparticles, then the unique photoluminescent properties, such as fluorescent narrowing, multicolor emission, tunable emission, and switchable emission, were reviewed, and finally other optoelectronic properties were also briefly presented.

Currently, the research on nanomaterials based on small organic compounds is still in its infancy, and much remains to be done in this area. In our opinion, several directions deserve to be paid special attention in the future. First, developing methods for the general fabrication of organic nanomaterials with desired morphologies and structures is still a key task, although some progress, adsorbent-assisted PVD for instance, has been made in previous studies. Second, for the property studies, the optical and photonic properties of single organic nanoparticles and single nanowires have attracted some attention in the last one or two years, however, we think more work is required. Third, the design and synthesis of molecules with unique optoelectronic properties and the controllable construction of nanostructures with deliberately designed molecules are a great challenge as well as an opportunity. In addition, theoretical calculation has proved to be an effective way to design target molecules and to explain the electron processes in this area, so we hope more and more theoretical chemists will participate in this promising direction. As to the application of organic nanomaterials, novel performances such as optical waveguides and optically/electrically pumped lasers are under investigation, and, equally, the fabrication of thin films and patterns[210] composed of the nanostructured building blocks on solid substrates is essential for the realization of practical devices.

Received: March 3, 2008
Published online:

[1] P. Ball, L. Garwin, *Nature* **1992**, *355*, 761.
[2] A. N. Goldstein, C. M. Echer, A. P. Alivisatos, *Science* **1992**, *256*, 1425.
[3] M. A. Reed, W. R. Frensley, R. J. Matyi, J. N. Randall, A. C. Seabaugh, *Appl. Phys. Lett.* **1989**, *54*, 1034.
[4] L. Lu, Y. Shen, X. Chen, L. Qian, K. Lu, *Science* **2004**, *304*, 422.
[5] A. P. Alivisatos, P. F. Barbara, A. W. Castleman, J. Chang, D. A. Dixon, M. L. Kline, G. L. McLendon, J. S. Miller, M. A. Ratner, P. J. Rossky, S. I. Stupp, M. I. Thompson, *Adv. Mater.* **1998**, *10*, 1297.

  

[6] *Nanomaterials: Synthesis, Properties and Applications* (Eds: A. S. Edelstein, R. C. Cammarata), Institute of Physics, Philadelphia, PA **1996**.
[7] Special issue on nanomaterials, *Chem. Mater.* **1996**, *8*, 1569.
[8] M. Bruchez, Jr, M. Moronne, P. Gin, S. Weiss, A. P. Alivisatos, *Science* **1998**, *281*, 2013.
[9] Y. Gu, I. L. Kuskovsky, M. Yin, S. O'Brien, G. F. Neumark, *Appl. Phys. Lett.* **2004**, *85*, 3833.
[10] A. Corma, *Chem. Rev.* **1997**, *97*, 2373.
[11] W. C. W. Chan, S. Nie, *Science* **1998**, *281*, 2016.
[12] C. P. Chan, Y. Bruemmel, M. Seydack, K. Sin, L. Wong, E. Merisko-Liversidge, D. Trau, R. Renneberg, *Anal. Chem.* **2004**, *76*, 3638.
[13] A. Schroedter, H. Weller, R. Eritja, W. E. Ford, J. M. Wessels, *Nano Lett.* **2002**, *2*, 1363.
[14] H. Gu, P. L. Ho, K. W. T. Tsang, L. Wang, B. Xu, *J. Am. Chem. Soc.* **2003**, *125*, 15702.
[15] S. Fafard, K. Hinzer, S. Raymond, M. Dion, J. McCaffrey, Y. Feng, S. Charbonneau, *Science* **1996**, *274*, 1350.
[16] H. Parala, H. Winkler, M. Kolbe, A. Wohlfart, R. A. Fischer, R. Schmechel, H. von Seggern, *Adv. Mater.* **2000**, *12*, 1050.
[17] A. H. Mueller, M. A. Petruska, M. Achermann, D. J. Werder, E. A. Akhadov, D. D. Koleske, M. A. Hoffbauer, V. I. Klimov, *Nano Lett.* **2005**, *5*, 1039.
[18] J. C. Johnson, H. Yan, R. D. Schaller, P. B. Petersen, P. Yang, R. J. Saykally, *Nano Lett.* **2002**, *2*, 279.
[19] Y. Wang, X. Xie, T. Goodson, III, *Nano Lett.* **2005**, *5*, 2379.
[20] H. Fan, Y. Lu, A. Stump, S. T. Reed, T. Baer, R. Schunk, V. Perez-Luna, G. P. López, C. J. Brinker, *Nature* **2000**, *405*, 56.
[21] S. Ghosh, A. K. Sood, N. Kumar, *Science* **2003**, *299*, 1042.
[22] R. F. Service, *Science* **2000**, *287*, 1902.
[23] C. B. Murray, D. J. Norris, M. G. Bawendi, *J. Am. Chem. Soc.* **1993**, *115*, 8706.
[24] A. P. Alivisatos, *Pure Appl. Chem.* **2000**, *72*, 3.
[25] U. Banin, Y. Cao, D. Katz, O. Millo, *Nature* **1999**, *400*, 542.
[26] X. Peng, L. Manna, W. Yang, J. Wickham, E. Scher, A. Kadavanich, A. P. Alivisatos, *Nature* **2000**, *404*, 59.
[27] W. W. Yu, L. Qu, W. Guo, X. Peng, *Chem. Mater.* **2003**, *15*, 2854.
[28] W. U. Huynh, X. Peng, A. P. Alivisatos, *Adv. Mater.* **1999**, *11*, 923.
[29] A. N. Shipway, E. Katz, I. Willner, *ChemPhysChem* **2000**, *1*, 18.
[30] I. H. Campbell, B. K. Crone, *Adv. Mater.* **2006**, *18*, 77.
[31] M. Kroutvar, A. Zrenner, Y. Ducommun, J. J. Finley, G. Abstreiter, *Phys. Status Solidi B* **2003**, *238*, 345.
[32] Y. C. Cao, R. Jin, C. A. Mirkin, *Science* **2002**, *297*, 1536.
[33] Y. Sun, Y. Xia, *Science* **2002**, *298*, 2176.
[34] F. Hu, L. Wei, Z. Zhou, Y. Ran, Z. Li, M. Gao, *Adv. Mater.* **2006**, *18*, 2553.
[35] W. S. Seo, J. H. Lee, X. Sun, Y. Suzuki, D. Mann, Z. Liu, M. Terashima, P. C. Yang, M. V. McConnell, D. G. Nishimura, H. Dai, *Nat. Mater.* **2006**, *5*, 971.
[36] S. Iijima, *Nature* **1991**, *354*, 56.
[37] X. Duan, Y. Huang, Y. Cui, J. Wang, C. M. Lieber, *Nature* **2001**, *409*, 66.
[38] M. Law, D. J. Sirbuly, J. C. Johnson, J. Goldberger, R. G. Saykally, P. Yang, *Science* **2004**, *305*, 1269.
[39] D. Golberg, Y. Bando, C. C. Tang, C. Y. Zhi, *Adv. Mater.* **2007**, *19*, 2413.
[40] R. E. Schaak, T. E. Mallouk, *Chem. Mater.* **2003**, *12*, 3427.
[41] W. U. Huynh, J. J. Dittmer, A. P. Alivisatos, *Science* **2002**, *295*, 2425.
[42] Z. W. Pan, Z. R. Dai, Z. L. Wang, *Science* **2001**, *291*, 1947.
[43] P. Yang, H. Yan, S. Mao, R. Russo, J. Johnson, R. Saykally, N. Morris, J. Pham, R. He, H. J. Choi, *Adv. Funct. Mater.* **2002**, *12*, 323.
[44] A. Pan, D. Liu, R. Liu, F. Wang, X. Zhu, B. Zou, *Small* **2005**, *1*, 980.
[45] C. J. Barrelet, A. B. Greytak, C. M. Lieber, *Nano Lett.* **2004**, *4*, 1981.
[46] J. C. Johnson, H.-J. Choi, K. P. Knutsen, R. D. Schaller, P. Yang, R. J. Saykally, *Nat. Mater.* **2002**, *1*, 106.
[47] Z. L. Wang, *Adv. Mater.* **2003**, *15*, 432.
[48] J. Hu, T. W. Odom, C. M. Lieber, *Acc. Chem. Res.* **1999**, *32*, 435.
[49] Y. Xia, P. Yang, Y. Sun, Y. Wu, B. Mayers, B. Gates, Y. Yin, F. Kim, H. Yan, *Adv. Mater.* **2003**, *15*, 353.
[50] M. Law, J. Goldberger, P. Yang, *Annu. Rev. Mater. Res.* **2004**, *34*, 83.
[51] M. A. Herman, H. Sitter, *Molecular Beam Epitaxy: Fundamentals and Current Status* (Springer Ser. Mater. Sci, Vol. 7), Springer, Berlin **1996**.
[52] P. Jiang, J. F. Bertone, K. S. Hwang, V. L. Colvin, *Chem. Mater.* **1999**, *11*, 2132.
[53] M. Okubo, H. Minami, K. Morikawa, *Colloid Polym. Sci.* **2003**, *281*, 214.
[54] K. Landfester, R. Montenegro, U. Scherf, R. Güntner, U. Asawapirom, S. Patil, D. Neher, T. Kietzke, *Adv. Mater.* **2002**, *14*, 651.
[55] C. Szymanski, C. Wu, J. Hooper, M. A. Salazar, A. Perdomo, A. Dukes, J. McNeill, *J. Phys. Chem. B* **2005**, *109*, 8543.
[56] P. Leclère, V. Parente, J. L. Brédas, B. François, R. Lazzaroni, *Chem. Mater.* **1998**, *10*, 4010.
[57] F. Chen, Y. Kondo, T. Hashimoto, *Macromolecules* **2007**, *40*, 3714.
[58] Z. X. Wei, L. J. Zhang, M. Yu, Y. S. Yang, M. X. Wan, *Adv. Mater.* **2003**, *15*, 1382.
[59] W. Zhong, S. Liu, X. Chen, Y. Wang, W. Yang, *Macromolecules* **2006**, *39*, 3224.
[60] J. Huang, S. Virji, B. H. Weiller, R. B. Kaner, *J. Am. Chem. Soc.* **2003**, *125*, 314.
[61] E. Smela, *Adv. Mater.* **2003**, *15*, 481.
[62] Y. Berdichevsky, Y.-H. Lo, *Adv. Mater.* **2006**, *18*, 122.
[63] N. J. Pinto, A. T. Johnson, Jr, A. G. MacDiarmid, C. H. Mueller, N. Theofylaktos, D. C. Robinson, F. A. Miranda, *Appl. Phys. Lett.* **2003**, *83*, 4244.
[64] D. O'Carroll, I. Lieberwirth, G. Redmond, *Nat. Nanotechnol.* **2007**, *2*, 180.
[65] G. A. O'Brien, A. J. Quinn, D. A. Tanner, G. Redmond, *Adv. Mater.* **2006**, *18*, 2379.
[66] M. Granström, M. Berggren, O. Inganäs, *Science* **1995**, *267*, 1479.
[67] K. Ramanathan, M. A. Bangar, M. Yun, W. Chen, A. Mulchandani, N. V. Myung, *Nano Lett.* **2004**, *4*, 1237.
[68] L. Wang, P. D. Topham, O. O. Mykhaylyk, J. R. Howse, W. Bras, R. A. L. Jones, A. J. Ryan, *Adv. Mater.* **2007**, *19*, 3544.
[69] Z. Wei, M. Wan, T. Lin, L. Dai, *Adv. Mater.* **2003**, *15*, 136.
[70] C. R. Martin, *Acc. Chem. Res.* **1995**, *28*, 61.
[71] H. Nakao, M. Gad, S. Sugiyama, K. Otobe, T. Ohtani, *J. Am. Chem. Soc.* **2003**, *125*, 7162.
[72] Z. Deng, C. Mao, *Nano Lett.* **2003**, *3*, 1545.
[73] M. A. Lapierre-Devlin, C. L. Asher, B. J. Taft, R. Gasparac, M. A. Roberts, S. O. Kelley, *Nano Lett.* **2005**, *5*, 1051.
[74] M. R. Ghadiri, J. R. Granja, R. A. Milligan, D. E. McRee, N. Khazanovich, *Nature* **1993**, *366*, 324.
[75] D. T. Bong, T. D. Clark, J. R. Granja, M. R. Ghadiri, *Angew. Chem. Int. Ed.* **2001**, *40*, 988.
[76] F. J. M. Hoeben, P. Jonkheijm, E. W. Meijer, A. P. H. J. Schenning, *Chem. Rev.* **2005**, *105*, 1491.
[77] A. C. Grimsdale, K. Müllen, *Angew. Chem. Int. Ed.* **2005**, *44*, 5592.
[78] D. Yan, Y. Zhou, J. Hou, *Science* **2004**, *303*, 65.
[79] Y. Kim, M. F. Mayer, S. C. Zimmerman, *Angew. Chem. Int. Ed.* **2003**, *42*, 1121.
[80] T. Yamaguchi, N. Ishii, K. Tashiro, T. Aida, *J. Am. Chem. Soc.* **2003**, *125*, 13934.
[81] T. Shimizu, M. Masuda, H. Minamikawa, *Chem. Rev.* **2005**, *105*, 1401.
[82] Y. Shinozuka, M. Matsuura, *Phys. Rev. B* **1983**, *28*, 4878.
[83] V. Vikhnin, S. Kapphan, *Phys. Solid State* **1998**, *40*, 834.

[84] M. Pope, C. E. Swenberg, *Electronic Processes in Organic Crystals and Polymers*, 2nd ed., Oxford University Press, Oxford **1999**.
[85] H. Kasai, H. S. Nalwa, H. Oikawa, S. Okada, H. Matsuda, N. Minami, A. Kakuta, K. Ono, A. Mukoh, H. Nakanishi, *Jpn. J. Appl. Phys.* **1992**, *31*, L1132.
[86] V. Chernyak, T. Meier, E. Tsiper, S. Mukamel, *J. Phys. Chem. A* **1999**, *103*, 10294.
[87] F. Spano, S. Umkamel, *Phys. Rev. A* **1989**, *40*, 5783.
[88] Q. Jiang, H. X. Shi, M. Zhao, *J. Chem. Phys.* **1999**, *111*, 2176.
[89] D. Horn, J. Rieger, *Angew. Chem. Int. Ed.* **2001**, *40*, 4330.
[90] M. F. Zambaux, F. Bonneaux, R. Gref, E. Dellacherie, C. Vigneron, *J. Controlled Release* **1999**, *60*, 179.
[91] M. T. Peracchia, C. Vauthier, D. Desmaële, A. Gulik, J. C. Dedieu, M. Demoy, J. d'Angelo, P. Couvreur, *Pharm. Res.* **1998**, *15*, 550.
[92] H. Murakami, M. Kobayashi, H. Takeuchi, Y. Kawashima, *Int. J. Pharm.* **1999**, *187*, 143.
[93] D. Quintanar-Guerrero, E. Allémann, E. Doelker, H. Fessi, *Colloid Polym. Sci.* **1997**, *275*, 640.
[94] B. Yu, Shekunov, P. York, *J. Cryst. Growth* **2000**, *211*, 122.
[95] S. Palakodaty, P. York, *Pharm. Res.* **1999**, *16*, 976.
[96] E. Donath, G. B. Sukhorukov, F. Caruso, S. Davis, H. Möhwald, *Angew. Chem. Int. Ed.* **1998**, *37*, 2201.
[97] F. Caruso, *Adv. Mater.* **2001**, *13*, 11.
[98] Y. Tamaki, T. Asahi, H. Masuhara, *J. Phys. Chem. A* **2002**, *106*, 2135.
[99] K. Baba, H. Kasai, S. Okada, H. Oikawa, H. Nakanishi, *Opt. Mater.* **2002**, *21*, 591.
[100] F. Debuigne, L. Jeunieau, M. Wiame, J. B. Nagy, *Langmuir* **2000**, *16*, 7605.
[101] Z. Jia, D. Xiao, W. Yang, Y. Ma, J. Yao, Z. Liu, *J. Membr. Sci.* **2004**, *241*, 387.
[102] H. S. Nalwa, H. Kasai, H. Kamatani, S. Okada, H. Oikawa, H. Matsuda, A. Kakuta, A. Mukoh, H. Nakanishi, *Adv. Mater.* **1993**, *5*, 758.
[103] H. Kasai, H. Oikawa, H. Nakanishi, *Organic Mesoscopic Chemistry* (Eds: H. Masuhara, F. C. Schryver), Blackwell Science, Oxford **1999**, pp. 145–170.
[104] H. Kasai, H. Kamatani, Y. Yoshikawa, S. Okada, H. Oikawa, A. Watanabe, O. Itoh, H. Nakanishi, *Chem. Lett.* **1997**, *26*, 1181.
[105] H. Oikawa, T. Mitsui, T. Onodera, H. Kasai, H. Nakanishi, T. Sekiguchi, *Jpn. J. Appl. Phys.* **2003**, *42*, L111.
[106] H. Auweter, H. Haberkorn, W. Heckmann, D. Horn, E. Lüddecke, J. Rieger, H. Weiss, *Angew. Chem. Int. Ed.* **1999**, *38*, 2188.
[107] T. Tachikawa, H.-R. Chung, A. Masuhara, H. Kasai, H. Oikawa, H. Nakanishi, M. Fujitsuka, T. Majima, *J. Am. Chem. Soc.* **2006**, *128*, 15944.
[108] A. J. Gesquiere, T. Uwada, T. Asahi, H. Masuhara, P. F. Barbara, *Nano Lett.* **2005**, *5*, 1321.
[109] F. Bertorelle, D. Lavabre, S. Fery-Forgues, *J. Am. Chem. Soc.* **2003**, *125*, 6244.
[110] L. Kang, Z. Wang, Z. Cao, Y. Ma, H. Fu, J. Yao, *J. Am. Chem. Soc.* **2007**, *129*, 7305.
[111] C. V. Ristagno, H. J. Shine, *J. Org. Chem.* **1971**, *36*, 4050.
[112] D. D. L. Chung, *Composite Materials: Functional Materials for Modern Technologies*, Springer, New York **2004**.
[113] J. Jang, J. H. Oh, *Adv. Mater.* **2003**, *15*, 977.
[114] W. T. S. Huck, J. Tien, G. M. Whitesides, *J. Am. Chem. Soc.* **1998**, *120*, 8267.
[115] Z. Wang, C. J. Medforth, J. A. Shelnutt, *J. Am. Chem. Soc.* **2004**, *126*, 15954.
[116] Z. Wang, C. J. Medforth, J. A. Shelnutt, *J. Am. Chem. Soc.* **2004**, *126*, 16720.
[117] K. Takazawa, Y. Kitahama, Y. Kimura, G. Kido, *Nano Lett.* **2005**, *5*, 1293.
[118] K. Takazawa, *J. Phys. Chem. C* **2007**, *111*, 8671.
[119] G. John, M. Masuda, Y. Okada, K. Yase, T. Shimizu, *Adv. Mater.* **2001**, *13*, 715.
[120] Y. S. Zhao, W. Yang, D. Xiao, X. Sheng, X. Yang, Z. Shuai, Y. Luo, J. Yao, *Chem. Mater.* **2005**, *17*, 6430.
[121] X. Zhang, X. Zhang, W. Shi, X. Meng, C. S. Lee, S. T. Lee, *Angew. Chem. Int. Ed.* **2007**, *46*, 1525.
[122] J. Wang, Y. Zhao, J. Zhang, J. Zhang, B. Yang, Y. Wang, D. Zhang, H. You, D. Ma, *J. Phys. Chem. C* **2007**, *111*, 9177.
[123] K. Balakrishnan, A. Datar, R. Oitker, H. Chen, J. Zuo, L. Zang, *J. Am. Chem. Soc.* **2005**, *127*, 10496.
[124] K. Balakrishnan, A. Datar, W. Zhang, X. Yang, T. Naddo, J. Huang, J. Zuo, M. Yen, J. S. Moore, L. Zang, *J. Am. Chem. Soc.* **2006**, *128*, 6576.
[125] Y. Che, A. Datar, K. Balakrishnan, L. Zang, *J. Am. Chem. Soc.* **2007**, *129*, 7234.
[126] P. Terech, R. G. Weiss, *Chem. Rev.* **1997**, *97*, 3133.
[127] J. H. van Esch, B. L. Feringa, *Angew. Chem. Int. Ed.* **2000**, *39*, 2263.
[128] A. Ajayaghosh, S. J. George, *J. Am. Chem. Soc.* **2001**, *123*, 5148.
[129] K. Yoza, Y. Ono, K. Yoshihara, T. Akao, H. Shinmori, M. Takeuchi, S. Shinkai, D. N. Reinhoudt, *Chem. Commun.* **1998**, *907*.
[130] J. H. Jung, S. Shinkai, T. Shimizu, *Chem. Eur. J.* **2002**, *8*, 2684.
[131] K. Hanabusa, M. Yamada, M. Kimura, H. Shirai, *Angew. Chem. Int. Ed.* **1996**, *35*, 1949.
[132] Y. Ono, K. Nakashima, M. Sano, K. Kanekiyo, K. Inoue, J. Hojo, S. Shinkai, *Chem. Commun.* **1998**, *1477*.
[133] B.-K. An, D.-S. Lee, J.-S. Lee, Y.-S. Park, H.-S. Song, S. Y. Park, *J. Am. Chem. Soc.* **2004**, *126*, 10232.
[134] Y. S. Zhao, W. Yang, J. Yao, *Phys. Chem. Chem. Phys.* **2006**, *8*, 3300.
[135] J. Chen, T. Herricks, M. Geissler, Y. Xia, *J. Am. Chem. Soc.* **2004**, *126*, 10854.
[136] Y. Liu, J. Cao, J. Zeng, C. Li, Y. Qian, S. Zhang, *Eur. J. Inorg. Chem.* **2003**, *4*, 644.
[137] H. A. Becerril, R. M. Stoltenberg, D. R. Wheeler, R. C. Davis, J. N. Harb, A. T. Woolley, *J. Am. Chem. Soc.* **2005**, *127*, 2828.
[138] C. Minelli, C. Hinderling, H. Heinzelmann, R. Pugin, M. Liley, *Langmuir* **2005**, *21*, 7080.
[139] M. J. Rosen, *Surfactants and Interfacial Phenomena*, 3rd ed., Wiley, New York **2004**.
[140] H. Fu, D. Xiao, J. Yao, G. Yang, *Angew. Chem. Int. Ed.* **2003**, *42*, 2883.
[141] J.-S. Hu, Y.-G. Guo, H.-P. Liang, L.-J. Wan, L. Jiang, *J. Am. Chem. Soc.* **2005**, *127*, 17090.
[142] X. Zhang, X. Zhang, W. Shi, X. Meng, C. Lee, S. Lee, *J. Phys. Chem. B* **2005**, *109*, 18777.
[143] C. R. Martin, *Science* **1994**, *266*, 1961.
[144] G. E. Possin, *Rev. Sci. Instrum.* **1970**, *41*, 772.
[145] T. Kim, I. Park, R. Ryoo, *Angew. Chem. Int. Ed.* **2003**, *42*, 4375.
[146] A. D. Berry, R. J. Tonucci, M. Fatemi, *Appl. Phys. Lett.* **1996**, *69*, 2846.
[147] S. K. Chakarvarti, J. Vetter, *Radiat. Meas.* **1998**, *29*, 149.
[148] J.-K. Lee, W. K. Koh, W.-S. Chaeb, Y.-R. Kim, *Chem. Commun.* **2002**, *138*.
[149] H. Liu, Y. Li, L. Jiang, H. Luo, S. Xiao, H. Fang, H. Li, D. Zhu, D. Yu, J. Xu, B. Xiang, *J. Am. Chem. Soc.* **2002**, *124*, 13370.
[150] L. Zhao, W. Yang, Y. Ma, J. Yao, Y. Li, H. Liu, *Chem. Commun.* **2003**, 2442.
[151] L. Zhao, W. Yang, Y. Luo, T. Zhai, G. Zhang, J. Yao, *Chem. Eur. J.* **2005**, *11*, 3773.
[152] Z. R. Dai, Z. W. Pan, Z. L. Wang, *Adv. Funct. Mater.* **2003**, *13*, 9.
[153] F. Balzer, V. G. Bordo, A. C. Simonsen, H.-G. Rubahn, *Appl. Phys. Lett.* **2003**, *82*, 10.
[154] J. J. Chiu, C. C. Kei, T. P. Perng, W. S. Wang, *Adv. Mater.* **2003**, *15*, 1361.
[155] H. Liu, Y. Li, S. Xiao, H. Gan, T. Jiu, H. Li, L. Jiang, D. Zhu, D. Yu, B. Xiang, Y. Chen, *J. Am. Chem. Soc.* **2003**, *125*, 10794.


  

[156] B. S. Ong, Y. L. Wu, P. Liu, S. Gardner, *J. Am. Chem. Soc.* **2004**, *126*, 3378.
[157] Y. S. Zhao, C. Di, W. Yang, G. Yu, Y. Liu, J. Yao, *Adv. Funct. Mater.* **2006**, *16*, 1985.
[158] Y. S. Zhao, D. Xiao, W. Yang, A. Peng, J. Yao, *Chem. Mater.* **2006**, *18*, 2302.
[159] Y. S. Zhao, H. Fu, F. Hu, A. Peng, J. Yao, *Adv. Mater.* **2007**, *19*, 3554.
[160] Y. S. Zhao, H. Fu, F. Hu, A. Peng, W. Yang, J. Yao, *Adv. Mater.* **2008**, *20*, 79.
[161] F. Kim, S. Connor, H. Song, T. Kuykendall, P. Yang, *Angew. Chem. Int. Ed.* **2004**, *43*, 3673.
[162] Z. W. Pan, S. Dai, C. M. Rouleau, D. H. Lowndes, *Angew. Chem. Int. Ed.* **2005**, *44*, 274.
[163] Z. Tian, Y. Chen, W. Yang, J. Yao, L. Zhu, Z. Shuai, *Angew. Chem. Int. Ed.* **2004**, *43*, 4060.
[164] A. D. L. Escosura, M. V. Martinez-Diaz, P. Thordarson, A. E. Rowan, R. J. M. Nolte, T. Torres, *J. Am. Chem. Soc.* **2003**, *125*, 12300.
[165] Y. Wang, H. Fu, A. Peng, Y. Zhao, J. Ma, Y. Ma, J. Yao, *Chem. Commun.* **2007**, *1623.*
[166] Y. S. Zhao, F. Hu, W. Yang, Y. Ma, H. Fu, J. Yao, *J. Nanosci. Nanotechnol.* **2007**, *7*, 1021.
[167] Y. Sun, Y. Yin, B. T. Mayers, T. Herricks, Y. Xia, *Chem. Mater.* **2002**, *14*, 4736.
[168] M. Li, H. Schnablegger, S. Mann, *Nature* **1999**, *402*, 393.
[169] Z. Tian, Y. Zhang, Y. Ma, W. Yan, Y. Chen, Y. Tang, J. Yao, *Colloids Surf. A* **2005**, *269*, 16.
[170] Y. S. Zhao, W. Yang, G. Zhang, Y. Ma, J. Yao, *Colloids Surf. A* **2006**, *277*, 111.
[171] Y. Liu, Z. Ji, Q. Tang, L. Jiang, H. Li, M. He, W. Hu, D. Zhang, L. Jiang, X. Wang, C. Wang, Y. Liu, D. Zhu, *Adv. Mater.* **2005**, *17*, 2953.
[172] H. Kasai, H. Kamatani, S. Okada, H. Oikawa, H. Matsuda, H. Nakanishi, *Jpn. J. Appl. Phys.* **1996**, *35*, L221.
[173] H. Fu, J. Yao, *J. Am. Chem. Soc.* **2001**, *123*, 1434.
[174] D. Xiao, L. Xi, W. Yang, H. Fu, Z. Shuai, Y. Fang, J. Yao, *J. Am. Chem. Soc.* **2003**, *125*, 6740.
[175] H. Fu, B. H. Loo, D. Xiao, R. Xie, X. Ji, J. Yao, B. Zhang, L. Zhang, *Angew. Chem. Int. Ed.* **2002**, *41*, 962.
[176] X. C. Gao, H. Cao, L. Q. Zhang, B. W. Zhang, Y. Cao, C. H. Huang, *J. Mater. Chem.* **1999**, *9*, 1077.
[177] D. Xiao, W. Yang, J. Yao, L. Xi, X. Yang, Z. Shuai, *J. Am. Chem. Soc.* **2004**, *126*, 15439.
[178] Z. Y. Tian, W. T. Huang, D. B. Xiao, S. Q. Wang, Y. S. Wu, Q. H. Gong, W. S. Yang, J. N. Yao, *Chem. Phys. Lett.* **2004**, *391*, 283.
[179] R. Deans, J. Kim, M. R. Machacek, T. M. Swager, *J. Am. Chem. Soc.* **2000**, *122*, 8565.
[180] J. Luo, Z. Xie, J. W. Lam, L. Cheng, H. Chen, C. Qiu, H. S. Kwok, X. Zhan, Y. Liu, D. Zhu, B. Z. Tang, *Chem. Commun.* **2001**, 1740.
[181] B.-K. An, S.-K. Kwon, S.-D. Jung, S. Y. Park, *J. Am. Chem. Soc.* **2002**, *124*, 14410.
[182] S.-J. Lim, B.-K. An, S. D. Jung, M.-A. Chung, S. Y. Park, *Angew. Chem. Int. Ed.* **2004**, *43*, 6346.
[183] A. Bloess, Y. Durand, M. Matsushita, R. Verberk, E. J. J. Groenen, J. Schmidt, *J. Phys. Chem. A* **2001**, *105*, 3016.
[184] R. Zallen, *The Physics of Amorphous Solids*, Wiley-Interscience, New York **1983**.
[185] Y. Durand, A. Bloeß, A. M. van Oijen, J. Köhler, E. J. J. Groenen, J. Schmidt, *Chem. Phys. Lett.* **2000**, *317*, 232.
[186] P. A. Lane, L. C. Palilis, D. F. O'Brien, C. Giebeler, A. J. Cadby, D. G. Lidzey, A. J. Campbell, W. Blau, D. D. C. Bradley, *Phys. Rev. B* **2001**, *63*, 235206.
[187] A. Pogantsch, G. Trattnig, G. Langer, W. Kern, U. Scherf, H. Tillmann, H. H. Hörhold, E. Zojer, *Adv. Mater.* **2002**, *14*, 1722.
[188] X.-C. Gao, H. Cao, L. Huang, Y.-Y. Huang, B.-W. Zhang, C.-H. Huang, *Appl. Surf. Sci.* **2003**, *210*, 183.
[189] A. B. Djurišić, Y. H. Leung, K. H. Tam, Y. F. Hsu, L. Ding, W. K. Ge, Y. C. Zhong, K. S. Wong, W. K. Chan, H. L. Tam, K. W. Cheah, W. M. Kwok, D. L. Philips, *Nanotechnology* **2007**, *18*, 095702.
[190] V. A. Lisovenko, M. T. Shpak, V. G. Antoniuk, *Chem. Phys. Lett.* **1976**, *42*, 339.
[191] C. W. Tang, S. A. VanSlyke, C. H. Chen, *J. Appl. Phys.* **1989**, *65*, 3610.
[192] J. Kido, K. Kimura, K. Nagai, *Science* **1995**, *267*, 1332.
[193] H. Mattoussi, H. Murata, C. D. Merritt, Y. Iizumi, J. Kido, Z. H. Kafafi, *J. Appl. Phys.* **1999**, *86*, 2642.
[194] A. D. Peng, D. B. Xiao, Y. Ma, W. S. Yang, J. N. Yao, *Adv. Mater.* **2005**, *17*, 2070.
[195] M. Sun, T. Pullerits, P. Kjellberg, W. J. D. Beenken, K. Han, *J. Phys. Chem. A* **2006**, *110*, 6324.
[196] R. Aroca, T. Del Cano, J. A. de Saja, *Chem. Mater.* **2003**, *15*, 38.
[197] D. Käfer, G. Witte, *Phys. Chem. Chem. Phys.* **2005**, *7*, 2850.
[198] M. Kytka, A. Gerlach, F. Schreiber, J. Kov‚áč *Appl. Phys. Lett.* **2007**, *90*, 131911.
[199] M. Irie, *Chem. Rev.* **2000**, *100*, 1685.
[200] H. Tian, S. J. Yang, *Chem. Soc. Rev.* **2004**, *33*, 85.
[201] T. B. Norsten, N. R. Branda, *Adv. Mater.* **2001**, *13*, 347.
[202] X. Sheng, A. Peng, H. Fu, Y. Liu, Y. S. Zhao, Y. Ma, J. Yao, *Nanotechnology* **2007**, *18*, 145707.
[203] S. Jalili,1 H. Rafii-Tabar, *Phys. Rev. B* **2005**, *71*, 165410.
[204] H. Liu, Q. Zhao, Y. Li, Y. Liu, F. Lu, J. Zhuang, S. Wang, L. Jiang, D. Zhu, D. Yu, L. Chi, *J. Am. Chem. Soc.* **2005**, *127*, 1120.
[205] Q. Tang, H. Li, M. He, W. Hu, C. Liu, K. Chen, C. Wang, Y. Liu, D. Zhu, *Adv. Mater.* **2006**, *18*, 65.
[206] K. Xiao, J. Tao, Z. Pan, A. A. Puretzky, I. N. Ivanov, S. J. Pennycook, D. B. Geohegan, *Angew. Chem. Int. Ed.* **2007**, *46*, 2650.
[207] F. Quochi, F. Cordella, A. Mura, G. Bongiovanni, F. Balzer, H.-G. Rubahn, *Appl. Phys. Lett.* **2006**, *88*, 041106.
[208] K. Takazawa, *Chem. Mater.* **2007**, *19*, 5293.
[209] Y. S. Zhao, A. Peng, H. Fu, Y. Ma, J. Yao, *Adv. Mater.* **2008**, *20*, 1661.
[210] B.-K. An, S.-K. Kwon, S. Y. Park, *Angew. Chem. Int. Ed.* **2007**, *46*, 1978.